

A UNIFIED APPROACH IN GPS ACCURACY
DETERMINATION STUDIES

by

Didem Öztürk

B.S., Geodesy and Photogrammetry Department

Yildiz Technical University, 2005

Submitted to the Kandilli Observatory and
Earthquake Research Institute in partial fulfillment of
the requirements for the degree of
Master of Science

Graduate Program in Geodesy

Boğaziçi University

2009

ACKNOWLEDGEMENTS

I am very grateful to my supervisor, Assist. Prof. Dr. Ugur Sanli for his endless support and encouragement for my study. Without his guidance and persistent help this thesis would not have been this smooth.

We are grateful to NASA's Jet Propulsion Laboratory for providing GIPSY OASIS II software and for satellite orbit and clock solution files. We also thank to Scripps Orbit and Permanent Array Centre (SOPAC) researchers for opening their archives to scientific activities worldwide.

I am also thankful to KOERI Geodesy Department for their hospitality and friendliness. I am as ever, especially indebted to my family, for their love and support throughout my life. I also wish to thank all my dear friends for their support and understanding during my study.

ABSTRACT

A UNIFIED APPROACH IN GPS ACCURACY DETERMINATION STUDIES

By the time GPS technology started to be used in Geodesy, it is much easier to reach the desired precision of point positioning. It is significantly a useful technique, thus one can easily predict the accuracy of GPS before a field survey and know about the quality of the observations that have been made on a reference point.

Parallel to the improvement of the GPS technology, predicting the accuracy over short and long baselines has really been an important discussion. There have been several studies dealing with precise point positioning and the topic was to determine how the accuracy depends on the baseline length and the duration of the observing session (Eckl *et al.*, 2001, Soler *et al.*, 2005, Doğan, 2007, Engin and Sanli, 2009).

In the previous studies, the accuracies for the baselines were taken into account separately, and models have been created for the baselines between 30-300 km and 300-3000 km. For the baselines smaller than 300 km, the accuracy was found to be a function of only the observing session duration (Eckl. *et al.*, 2001) but for the baselines between 300-3000 km the results show that it does not only depend on the observing session it also depends on the inter-station distance (Engin and Sanli, 2009).

In this study, the aim was to make the discussion topic certain and to combine a model for baselines ranging from 3 km to 3000 km. To define a unified model, GPS accuracy was tested in IGS network and the results are compared with recent studies by using GIPSY software. 13 baselines and the data of 10 days have been used in this research. Baseline lengths were between 3 km and 2739 km. The data of each day have been divided into sub sessions (6-8-12 and 24 hours) and then evaluated separately. Thus, the relation among GPS point positioning, base length and duration of observation has been examined.

The results show that, the point positioning accuracy in IGS network over 3-3000 km depends both on the baseline length and the observing session duration. It is partially possible to define a unified model for baselines between 3 and 3000 km. To define a unified model for this range, could only be possible by testing out the significance of various sub sets of Least Squares coefficients.

ÖZET

GPS DOĞRULUK ÇALIŞMALARINA BİRLEŞİK BİR YAKLAŞIM

GPS tekniklerinin jeodezik alanlarda kullanılmaya başlamasıyla beraber hedeflenen doğrulukta konum belirleyebilmek çok daha kolay hale gelmiştir. Araziye çıkmadan GPS doğruluğunu belirleyebilmek ve bir referans noktasında toplanmış verinin kalitesi hakkında fikir sahibi olabilmek yine GPS tekniklerini kullanarak mümkündür.

GPS teknolojisinin gelişmesine paralel olarak, kısa ve uzun bazlarda GPS doğruluğunun prediksyonuna yönelik çalışmalar önem kazanmıştır. Konum belirleme doğruluğu üzerine bir çok araştırma yapılmış ve bu araştırmalarda GPS doğruluğunun baz uzunluğuna ve gözlem süresine bağlılığı tartışılmıştır (Eckl *vd.*, 2001, Soler *vd.*, 2005, Doğan, 2007, Engin ve Sanli, 2009).

Önceki çalışmalarda doğruluğun gözlem süresi ve baz uzunluğuna bağlılığı kısa ve uzun bazlar için ayrı ayrı değerlendirilmiş ve 30-300 km uzunluğundaki bazlar ile 300-3000 km uzunluğundaki bazlar için farklı dengeleme modelleri yaratılmıştır. Sonuç olarak 300 km den kısa bazlar için doğruluğun yalnızca gözlem süresinin bir fonksiyonu olduğu (Eckl *vd.*, 2001) fakat 300-3000 km arasındaki bazlar için doğruluğun hem gözlem süresi hem de baz uzunluğuna bağlı olarak değiştiği ifade edilmiştir (Engin ve Sanli, 2009).

Bu çalışmada bizim amacımız GPS doğruluğu hakkında yapılan araştırmalara farklı bir ışık tutmak ve kısa ve uzun bazlar için ayrı ayrı oluşturulan modelleri, 3-3000 km lik bazlar için tek bir model haline dönüştürmektir. Bunun için, GPS doğruluğu IGS ağı sıklığında GIPSY yazılımı kullanılarak test edildi ve elde edilen sonuçlar bu konuda daha önceden gerçekleştirilen çalışmaların sonuçlarıyla karşılaştırıldı. Çalışmamızda uzunlukları 3 km ile 2739 km arasında değişen 13 baz ve bu bazlara ait 10 günlük data kullanıldı. Her güne ait 24 saatlik veriler 6, 8 ve 12 saatlik zaman dilimlerine bölünüp ayrı ayrı değerlendirildi ve GPS doğruluğu, gözlem süresi ve baz uzunluğu arasındaki ilişki incelendi.

Sonuç olarak IGS ağı kapsamında değerlendirilen 3-3000 km arasındaki bazlar için GPS doğruluğunun hem gözlem süresine hem de baz uzunluğuna bağlı olarak değiştiğini gözlemlendi. Bu aralıktaki veriyi tek bir model altında birleştirmenin kısmen mümkün olduğunu fakat bunun ancak anlamlı dengeleme katsayılarının farklı kombinasyonlarının test edilerek elde edilebileceğini gördük.

TABLE OF CONTENTS

ACKNOWLEDGEMENTS.....	iii
ABSTRACT.....	iv
ÖZET	vi
LIST OF FIGURES	ix
LIST OF TABLES.....	xiii
LIST OF SYMBOLS / ABBREVIATIONS.....	xiv
1. INTRODUCTION	1
2. ACCURACY OF GPS AND ERROR SOURCES.....	4
2.1. System Related Errors	5
2.2. Environmental Errors	6
2.3. User Related Errors.....	7
2.4. Other Error Sources	7
3. MISSION PLANNING.....	8
4. PRECISE POINT POSITIONING AND GIPSY OASIS II	9
5. STUDIES IN THE FIELD OF DETERMINING GPS ACCURACY	12
6. PREPERATION AND PROCESSING THE GPS DATA.....	18
7. APPLICATION	19
7.1. Aim of the Application	19
7.2. Computing RMS Values.....	19
7.3. Least Square Estimation	47
8.CONCLUSION.....	53
REFERENCES	55
AUTOBIOGRAPHY	57

LIST OF FIGURES

Figure 2.1.1.	Good GDOP and poor GDOP	5
Figure 2.2.1.	Environmental error sources and multipath effect	6
Figure 4.1.	Precise absolute coordinates can be obtained for a single receiver without the need for a second receiver.....	9
Figure 5.1.	RMS values for each baseline and each value of T according to Eckl <i>et al.</i> (2001).....	13
Figure 5.2.	Distribution of differences between estimated positions of the unknown points and their corresponding true positions acc. to Eckl <i>et al.</i> (2001)..	14
Figure 5.3.	Root Mean Square values for each baseline and each value of T according to Dogan (2007).....	16
Figure 5.4.	Solutions plotted against the predicted curve by Eckl <i>et al.</i> upper and lower bounds of the prediction are given with the dashed lines (Engin and Sanli 2009)	17
Figure 6.1.	Permanent GPS stations used in the study	18
Figure 7.2.1.	RMS values of north direction for the PADO-VOLT baseline.....	24
Figure 7.2.2.	RMS values of north direction for the SFEL- VENE baseline	24
Figure 7.2.3.	RMS values of north direction for the VOLT- VENE baseline	25
Figure 7.2.4.	RMS values of north direction for the SFEL-MEDI baseline.....	25

Figure 7.2.5.	RMS values of north direction for the BRAS-VOLT baseline	26
Figure 7.2.6.	RMS values of north direction for the CAVA-HFLK baseline.....	26
Figure 7.2.7.	RMS values of north direction for the SJDV-GRAS baseline	27
Figure 7.2.8.	RMS values of north direction for the MORP-HELG baseline	27
Figure 7.2.9.	RMS values of north direction for the HOBV-BRAS baseline.....	28
Figure 7.2.10.	RMS values of north direction for the LAMA-ZIMM baseline.....	28
Figure 7.2.11.	RMS values of north direction for the HELG-GLSV baseline	29
Figure 7.2.12.	RMS values of north direction for the ACOR-GRAZ baseline	29
Figure 7.2.13.	RMS values of north direction for the SODA-GENO baseline	30
Figure 7.2.14.	Relationship between RMS values of north direction, L and T	30
Figure 7.2.15.	RMS values of east direction for the PADO-VOLT baseline	32
Figure 7.2.16.	RMS values of east direction for the SFEL-VEVE baseline.....	32
Figure 7.2.17.	RMS values of east direction for the VOLT-VEVE baseline	33
Figure 7.2.18.	RMS values of east direction for the SFEL-MEDI baseline	33
Figure 7.2.19.	RMS values of east direction for the BRAS-VOLT baseline	34
Figure 7.2.20.	RMS values of east direction for the CAVA-HFLK baseline.....	34
Figure 7.2.21.	RMS values of east direction for the SJDV-GRAS baseline	35

Figure 7.2.22.	RMS values of east direction for the MORP-HELG baseline.....	35
Figure 7.2.23.	RMS values of east direction for the HOBU-BRAS baseline.....	36
Figure 7.2.24.	RMS values of east direction for the LAMA-ZIMM baseline.....	36
Figure 7.2.25.	RMS values of east direction for the HELG-GLSV baseline	37
Figure 7.2.26.	RMS values of east direction for the ACOR-GRAZ baseline.....	37
Figure 7.2.27.	RMS values of east direction for the SODA-GENO baseline.....	38
Figure 7.2.28.	Relationship between RMS values of east direction, L and T	38
Figure 7.2.29.	RMS values of up direction for the PADO-VOLT baseline	40
Figure 7.2.30.	RMS values of up direction for the SFEL-VE NE baseline.....	40
Figure 7.2.31.	RMS values of up direction for the VOLT-VE NE baseline	41
Figure 7.2.32.	RMS values of up direction for the SFEL-MEDI baseline	41
Figure 7.2.33.	RMS values of up direction for the BRAS-VOLT baseline.....	42
Figure 7.2.34.	RMS values of up direction for the CAVA-HFLK baseline	42
Figure 7.2.35.	RMS values of up direction for the SJDV-GRAS baseline.....	43
Figure 7.2.36.	RMS values of up direction for the MORP-HELG baseline.....	43
Figure 7.2.37.	RMS values of up direction for the HOBU-BRAS baseline.....	44

Figure 7.2.38.	RMS values of up direction for the LAMA-ZIMM baseline	44
Figure 7.2.39.	RMS values of up direction for the HELG-GLSV baseline.....	45
Figure 7.2.40.	RMS values of up direction for the ACOR-GRAZ baseline.....	45
Figure 7.2.41.	RMS values of up direction for the SODA-GENO baseline.....	46
Figure 7.2.42.	Relationship between RMS values of east direction, L and T	46
Figure 7.3.1.	RMS errors and curves fit according to LSE for the north component...	49
Figure 7.3.2.	RMS errors and curves fit according to LSE for the up component	49
Figure 7.3.3.	RMS errors and curves fit according to LSE for the east component.....	50

LIST OF TABLES

Table 7.2.1.	Names and the lengths of the baselines used in the study	20
Table 7.2.2.	RMS values of north, east and up for each baseline and each value of T .	22
Table 7.2.3.	Root mean square values (mm) of each baseline for north direction	23
Table 7.2.4.	Root mean square values (mm) of each baseline for east direction	31
Table 7.2.5.	Root mean square values (mm) of each baseline for up direction.....	39
Table 7.3.1.	Mean RMS values for alternative coefficient combinations for all three GPS baseline components north, east and up	51
Table 7.3.2.	Estimated values of constants in Equation (7.3.1).....	51
Table 7.3.3.	Mean RMS for all 13 baselines	52

LIST OF SYMBOLS / ABBREVIATIONS

SOPAC	Scripps Orbit and Permanent Array Center
GPS	Global Positioning System
IGS	International Geodetic System
NASA	National Aeronautics and Space Administration
SLR	Satellite Laser Ranging
JPL	Jet Propulsion Laboratory
EUREF	European Reference Frame
PPP	Precise Point Positioning
RMS	Root Mean Square
ITRF	International Terrestrial Reference Frame
LS	Least Squares

1. INTRODUCTION

With the rapid advancement of technology in today's world there have been many changes in the GPS industry. GPS has entirely changed the point of view of surveyors, engineers and the civilian population and it is now a common used technology for many sciences. GPS offers greater accuracy than traditional surveying techniques and today the precision of point locations is obtained in mm level.

After the GPS became a used technique in geodesy the GNSS services has been built. Today, the IGS products are practically used. More than this, one does not have to make an observation to get the data because it is possible to obtain GPS data through the internet (*i.e.* from SOPAC archives) which is a real advantage.

Parallel to the improvement of GPS technology, the studies evaluating the accuracy of GPS is more significant. Many GPS studies are carried out over short and long baselines to get empirical formulas for the dependency of accuracy. However, it is an uncertain topic whether these formulas can be combined to predict GPS accuracy over baselines of 1 to 3000 km. In this regard, firstly the studies that were carried out previously will be given in details in the next paragraphs.

Eckl *et al.*, (2001) processed 10 days of GPS data from 1998 by using PAGES software. Their aim was to determine how the accuracy of a derived three-dimensional relative position vector between GPS antennas depends on the chord distance (denoted L) between these antennas and on the duration of the GPS observing session (denoted T). It was found that the dependency of accuracy on L is negligibly small when using the final GPS satellite orbits, fixing integer ambiguities, estimating appropriate neutral-atmosphere-delay parameters. These experiments were carried out for L ranging between 26-300 km and T varying 4h – 24 h. The formulas that are created as a result of this research can be

used for the baselines shorter than 300 km, and it has been noticed that the accuracy is only a function of T when above conditions are provided.

Ozer, (2004) has studied on the baselines longer than 500 km. Two days of GPS data has been processed by using Bernese 4.2 software. As a conclusion, he has found that 4 hour observation was enough to get ± 1 cm accuracy between the baselines 500 km and 800 km. He kept the session duration fixed and tried to get the same accuracy over longer baselines. However, this time the errors were increased to 4-4,5 cm. Finally he proved that the accuracy was dependent on the baseline length as much as it was dependent on the session duration.

Soler *et al.*, (2005) noted the empirical formulas given in Eckl *et al.*, (2001) fail since fixing ambiguities becomes difficult for data spans shorter than 3 hours. Furthermore outliers in data increase due to multipath, poor satellite-receiver geometry and tropospheric anomalies.

Doğan, (2007) has almost used a similar data sample as Eckl. *et al.*, (2001) did. In his study, the observations made in Marmara Continuous GPS network was analysed. Seven days of GPS observations were collected and processed in the ITRF 2000 reference frame using Bernese 4.2 software. The baseline length varies between 6 km and 340 km and the session duration varies between 4 h and 24 h. The results of his study indicate that the accuracy of an observed relative position in the north-south, east-west and in the up-down directions depends significantly on both L (the chord distance) and T (session duration).

Engin and Sanli, (2009) aimed to assess GPS accuracies over longer baselines ranging from 300 km to 3000 km. 10 days of GPS data, taken from the permanent GPS stations, were obtained from the EUREF network and IGS through SOPAC archives. Each day's data were subdivided into mutually non-overlapping sessions for each several selected values of the observing session T (4, 6, 8, 12 and 24 h). And after processing the

data and examining the results, they have concluded that GPS positioning accuracy over regional scales depends both on the observing session duration and on the inter-station distance.

In this study, our aim has been to study the accuracy of GPS which covers both short and long baselines. We tried to combine the two models that were expressed by Eckl. *et al.*, (2001) over short baselines (*i.e.* 30-300 km) and Engin and Sanli, (2009) over long baselines (*i.e.* 300-3000 km).

We have summarized the previous studies carried out on the GPS accuracy field in the introduction part. In the second part of our study, accuracy of GPS and GPS error sources are detailed. Third part is the mission planning which gives us clues about how to plan a GPS survey. Then the next part answers what precise point positioning is and how GIPSY/OASIS II software processes the GPS data. The previous studies in the field of determining GPS accuracy are given in details in the fifth part of thesis. The next part is about the preparation and processing of the GPS data. The application is detailed in the seventh part, and the conclusions are given in the eight part.

2. ACCURACY OF GPS AND ERROR SOURCES

Today GPS is preferred to many conventional and space techniques since, visibility of ground points is not a problem, it works under all-weather conditions and it is suitable for global geophysical research. GPS is being used in establishing geodetic control networks, deformation monitoring of dams, bridges and highways, surveying applications in rural areas and monitoring of crustal motions, sea level rise and earth rotation.

Since GPS is a commonly used surveying technique for critical surveys, to understand the accuracy of the observations become more important. If we define the meaning of accuracy for GPS; it is the degree of conformance between the estimated or measured position, time and/or velocity of a GPS receiver and its true time, position and/or velocity as compared with a constant standard.

Although it is easier to obtain high precision by using GPS, there are some error sources that effect the accuracy such as system environmental problems, system related and user related errors. To avoid most affects that cause errors, continuous (24 hours) GPS observations must be collected. As the time passes, satellite geometry changes and it comes back to the first position by the end of 24 hours. For the observations less than 24 hours, the error sources are more effective on the accuracy. Because of that reason, it is going to be useful to examine these error sources in detail before going through the experimental part of thesis (Blewitt, 1997, Stewart and Rizos, 2002).

2.1. System Related Errors

GPS satellites are always in positive hemisphere so they can be viewed in the same direction. As a consequence there are no constraints from the southern direction. Thus shortening and lengthening of the GPS signal directly affects height estimation.

Satellite-receiver geometry is considered to be a system related error as well. During the observation, it is quite important that GPS receiver must see 4 satellites at all times. When visible GPS satellites are close together in the sky, the geometry is said to be weak and the DOP (dilution of precision) value is high; when far apart, the geometry is strong and the DOP value is low. Thus a low DOP value represents a better GPS positional accuracy due to the wider angular separation between the satellites used to calculate a GPS unit's position. Other factors that cause high DOP values are obstructions such as nearby mountains or buildings.

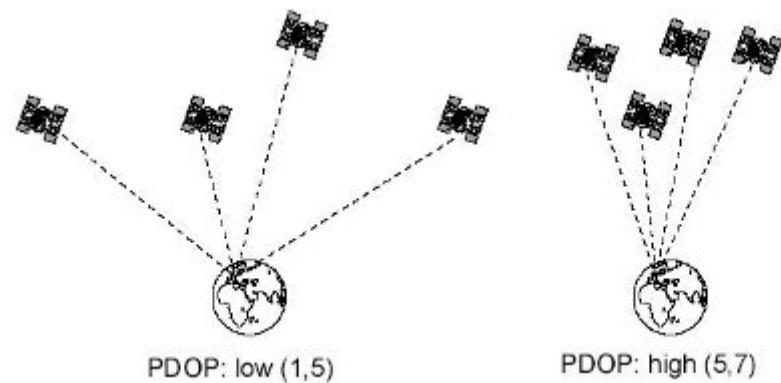


Figure 2.1.1. Good GDOP and poor GDOP

2.2. Environmental Errors

Especially for the observations made in the cities, it is risky to locate the GPS receiver close to some error sources such as buildings, trees, vehicles etc. For example, a building can block GPS signal coming from the satellite or the signal can be reflected because of the building and then come to the receiver. Both situations are unwanted cases for the accuracy.

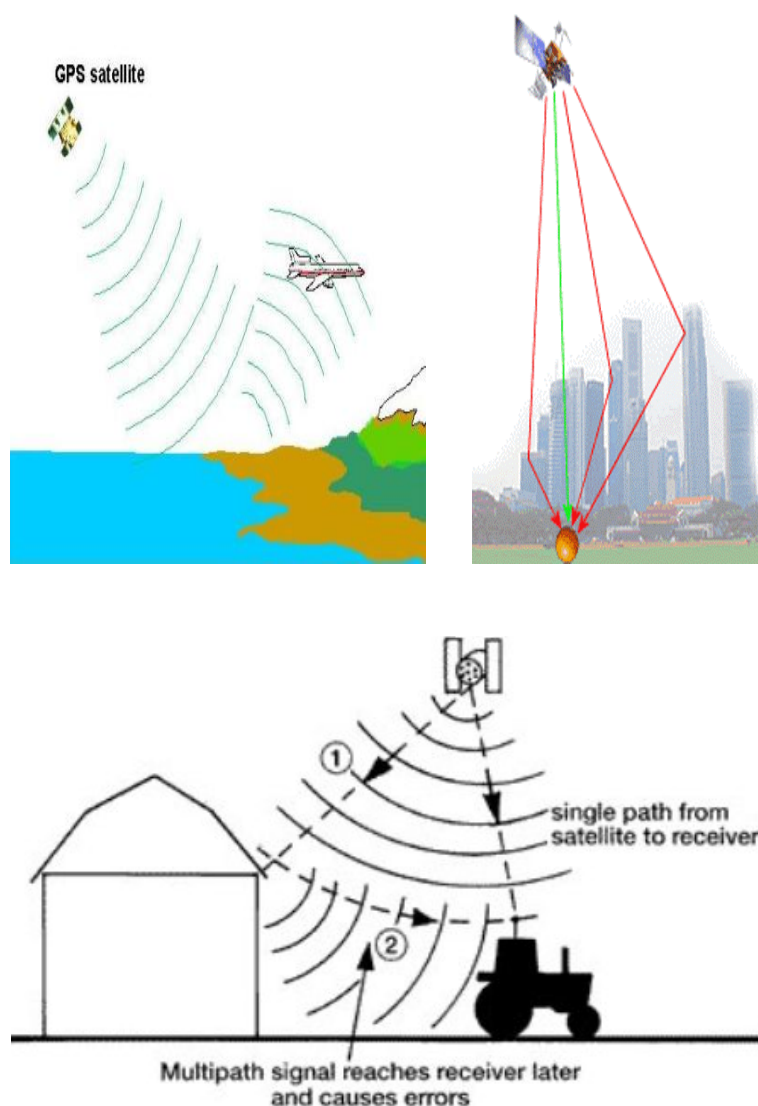


Figure 2.2.1. Environmental error sources and multipath effect

2.3. User Related Errors

People can make mistakes at measuring antenna heights and to avoid this, precise rods should be used, measurements should be taken from three sides of the antenna and the values should be recorded carefully. Antenna phase center variations can cause errors as well. Because phase centers are different among various antenna brands and to avoid this, same type of antennas should be used and antenna phase center parameters should be considered at processing.

2.4. Other Error Sources

Other error sources that effect accuracy can be listed as

- Atmospheric signal delays
- Ocean loading
- Hydrological cycle

3. MISSION PLANNING

For a higher precision, GPS surveys must be planned appropriately. Therefore, the right day and time gap can be worked out in the office to have good satellite geometry. To archive that, a GPS software and almanac data taken from the navigation message is used. Simply cofactor matrix is computed using approximate geographical location and coordinates of satellites estimated using the almanac data. Plotting the DOP values against time, one can obtain a chart illustrating good and bad satellite geometry in the future. Thus a good time span could be chosen for GPS observations in the office. By making 15 minute observation on a station it is possible to get next day's satellite geometry by 4 minutes difference.

When planning GPS measurements the following factors should be taken into consideration:

- Elevation angle must be chosen at least 15° to remove multipath and to prevent cycle-slips
- Right time gap must be determined for the best satellite geometry
- The most reliable and healthy satellites must be used

4. PRECISE POINT POSITIONING AND GIPSY/OASIS II

PPP is explained as the vast majority of commercially available software utilises the principles of relative positioning. However, in the late 1990s, the Jet Propulsion Laboratory (NASA) pioneered a new technique that did not require differencing to obtain precise positions. They labelled it Precise Point Positioning (PPP) and implemented it in their GIPSY/OASIS II GPS processing software. The largest difference between relative processing and PPP is the way that the satellite and receiver clock errors are handled.

Instead of between-receiver differencing to remove the satellite clock errors, PPP uses highly precise satellite clock estimates. These satellite clock estimates are derived from a solution using data from a globally distributed network of GPS receivers. Instead of between-satellite differencing to remove receiver clock errors, PPP estimates these as part of the least squares solution for the coordinates. Consequently, precise absolute coordinates for a single receiver at an unknown location may be obtained without the need of a second receiver at a known location.

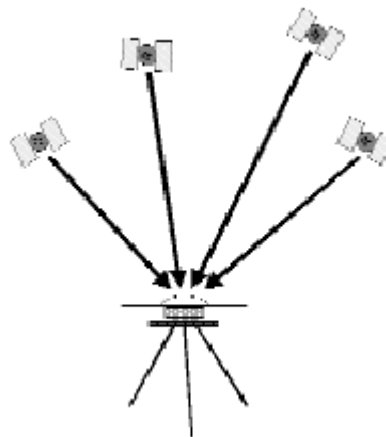


Figure 4.1. Precise absolute coordinates can be obtained for a single receiver without the need for a second receiver

A note of caution at this point is necessary. It may be possible to get PPP confused with another form of point positioning that many GPS users will be familiar with, *i.e.*, Single Point Positioning (SPP). SPP is different to PPP in two ways. Firstly, SPP does not use precise satellite clock values and secondly, only the pseudo range observations are used. PPP uses both the pseudo range and more precise carrier phase observations. The difference between these methods in terms of coordinate accuracy is large: SPP produces coordinates accurate at the 1-10 m level while PPP can produce coordinates accurate at the 0.01 m level with 24 hours of observations. Consequently, PPP allows coordinate determination with a precision that is comparable to relative processing. Since no base station is required in PPP, a further question is: “what datum are the coordinates in?” For PPP, the datum is hidden in the satellites’ coordinates – the satellite reference frame (datum) will be the unknown ground site reference frame. This means that to obtain coordinates in a different reference frame the user needs to perform a usually straightforward coordinate transformation (King *et al.*, 2002).

In other words, PPP is a new high precision mode of GPS positioning developed by NASA’s Jet Propulsion Scientists (Zumberge, 1997). It provides less than 1 cm accuracy with a single receiver and without any ground control. It has been developed as a quick alternative way to process huge amount of data. Precise point positioning is based on the idea that once we have precise orbits and clock information from some other source, we can position ourselves very accurately. IGS is the organization who currently provides such accurate orbits and clocks from a global network of GPS stations. Precise orbit and clock information (*i.e.*, *.eci, *.shad, *.tpeo.nml, *.tdpc files) can be obtained from JPL ftp site.

Recently research softwares such as BERNESSE, GAMIT and GIPSY are used for high precision point positioning. Ozer, (2005) and Dogan, (2007) have used BERNESSE 4.2 software in their study in order to examine the effect of observing session duration and baseline length on the accuracy. In our study GIPSY/OASIS II software, which has a completely different working principle from BERNESSE, is used. For that reason giving details about GIPSY software is going to be useful.

GIPSY/OASIS II is a high precision GPS point positioning software developed by NASA's Jet Propulsion Laboratory Scientists. It was initially developed to process GPS data however recently SLR, TOPEX and DORIS observations can be processed as well. It runs on the UNIX operation system (Webb and Zumberge, 1993, Gregorius, 1996).

GIPSY/OASIS II is a new high precision mode Precise Point Positioning (Zumberge, 1997) and can process data in all modes from static to kinematic, requiring only a single receiver. GIPSY does not use double differencing, instead clock parameters are estimated along with the geodetic parameters, processing undifferenced carrier phase and pseudorange data simultaneously (Blewitt, 1997). Clocks are estimated stochastically using white noise estimation that allows parameters vary from one batch of data to the next with a priori correlation between batches. Tropospheric zenith delay is estimated stochastically by random walk model (Tralli, 1990) which closely relates to the expected physics of atmospheric turbulence (Treuhaft, 1987).

5. STUDIES IN THE FIELD OF DETERMINING GPS ACCURACY

Eckl *et al.*, (2001) processed 10 days of GPS data from 1998 by using PAGES software. The aim of this study was to determine how the accuracy of a derived three-dimensional relative position vector between GPS antennas depends on the chord distance (denoted L) between these antennas and on the duration of the GPS observing session (denoted T). In the study, the final GPS satellite orbits determined by IGS were used, integer ambiguities were fixed and appropriate neutral-atmosphere-delay parameters were estimated. Baseline lengths changed between 26-300 km and the duration of the observing session was between 4-24 hours. As a result, it was found that the dependence of accuracy on L is negligibly small. Here, we see the general functional model below which is created by Eckl *et al.*, (2001).

$$S_n(L, T) = [a_n / T + b_n L^2 / T + c_n + d_n L^2]^{0,5} \quad (5.1)$$

Here a_n, b_n, c_n, d_n are the constants to be estimated using LS. The standard error can be represented by the square root of the sum of these four terms. The formulas that are created as a result of this research can be used for the baselines shorter than 300 km, and it has been emphasized that the accuracy is only a function of T when above conditions are provided. By using these formulas RMS values in all directions could be determined adequately accurate.

$$S_n = k_n / T^{0,5} \quad k_n = 9,5 \pm 2,1 \text{ mm.h}^{0,5} \quad (5.2)$$

$$S_e = k_e / T^{0,5} \quad k_e = 9,9 \pm 3,1 \text{ mm.h}^{0,5} \quad (5.3)$$

$$S_u = k_u / T^{0,5} \quad k_u = 36,5 \pm 9,1 \text{ mm.h}^{0,5} \quad (5.4)$$

Here S_n is equal to the RMS value on the north-south direction, S_e is the RMS value on the east-west direction and S_u is the RMS value on the up-down direction. k is a free parameter used instead of \sqrt{a} and T is expressed in hours.

When the duration of the observing session is assumed as 10 the RMS values are calculated for all directions. These values are $S_n=3$ mm, $S_e=3$ mm and $S_u=12$ mm which means the accuracy on horizontal direction is 3 mm and vertical direction is 12 mm when T is 10 hours.

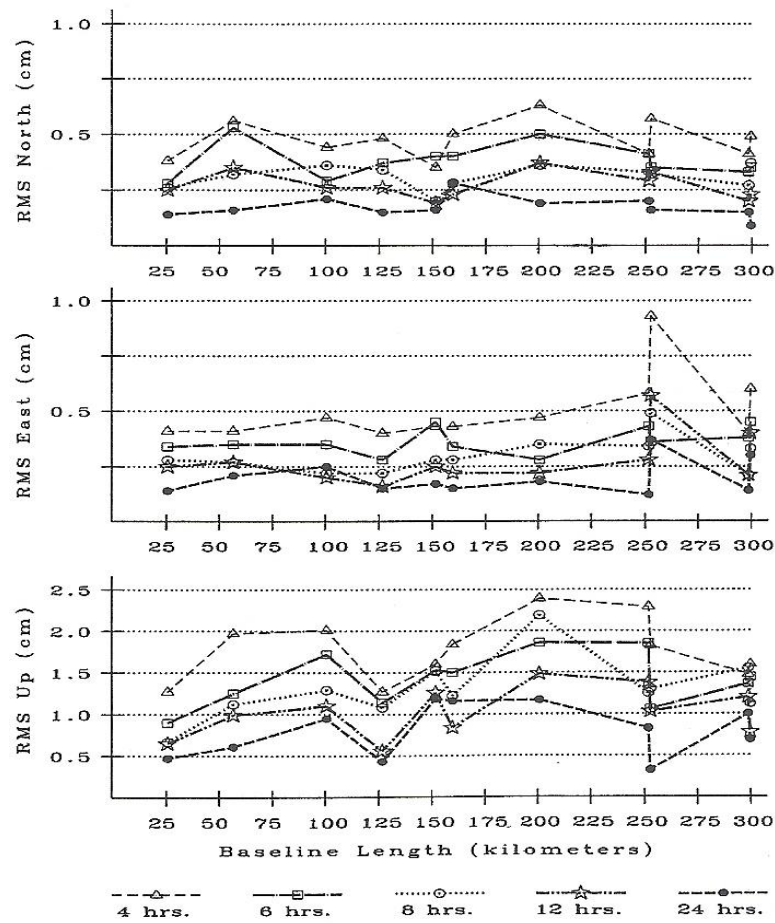


Figure 5.1. RMS values for each baseline and each value of T according to Eckl *et al.*, (2001)

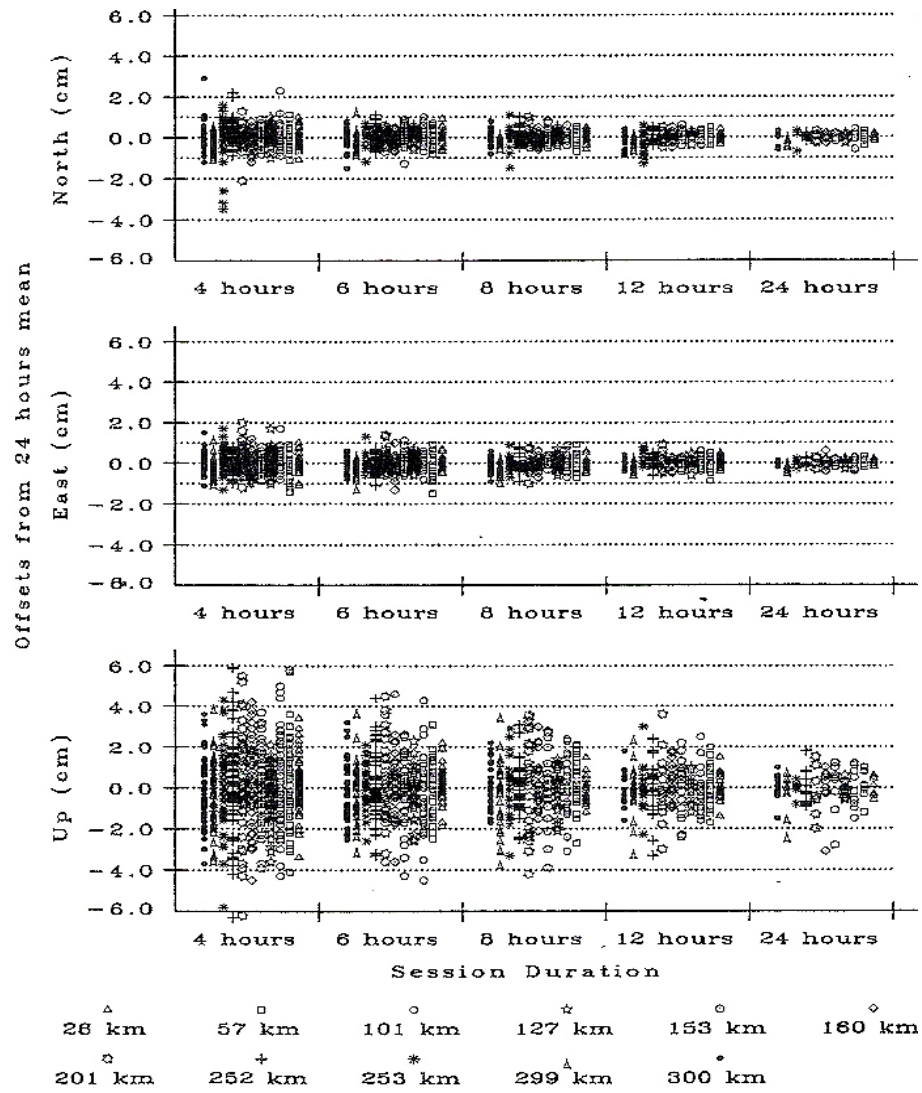


Figure 5.2. Distribution of differences between estimated positions of the unknown points and their corresponding true positions according to Eckl *et al.*, (2001)

Soler *et al.*, (2006) also studied the GPS accuracy by using Eckl *et al.*, (2001) model and they have studied on the observations where T was shorter. Eventually they have found that Eckl's model was not appropriate for the shorter observing sessions (*i.e.* less than 3 hours). It was because it is impossible to avoid multipath, tropospheric delays and it was hard to get the right satellite-receiver geometry over short observation sessions.

In the study of Dogan, (2007) the dependence of GPS accuracy was examined over the baselines between 6 km and 340 km which is a similar data sampling to Eckl *et al.*, (2001). T was between 4 and 24 hours and seven days of GPS observations were collected and processed in the ITRF 2000 reference frame using Bernese 4.2 software. The results of his study indicate that the accuracy of an observed relative position depends significantly on both L (the chord distance) and T (session duration). The results were different from the results presented in Eckl *et al.*, (2001) since Doğan, (2007) used another software for the processing and his data distribution was not homogeneous over the longer baselines compared to the short ones. These conditions (*i.e.* improper sampling of baseline lengths as well as the processing strategy) might affect the statistical significance of the results (Engin and Sanli, 2009).

Engin and Sanli, (2009) aimed to assess GPS accuracies over longer baselines. 10 days of GPS data covering the baselines between 300 and 3000 km were used in this study. Each day's data were subdivided into several selected values of the observing session T (4, 6, 8, 12 and 24 h). GIPSY/OASIS II software was used to process the GPS data. According to their study -where another software is used and longer baselines were examined- the results were similar to that of Eckl *et al.*, (2001) up to 2000 km. For the longer baselines the empirical formulas of Eckl *et al.*, (2001) do not represent well the accuracies in this range. Then new improved constants were estimated that fit best into their solutions. As a conclusion, the results differs from the findings of Eckl *et al.*, (2001) in that the accuracy of GPS positioning depends not only on the observing session duration but also on the inter-station distance. They have added that the result is somehow expected since they work on longer baselines and over longer baselines, atmospheric modeling errors and satellite orbit errors start to become significant.

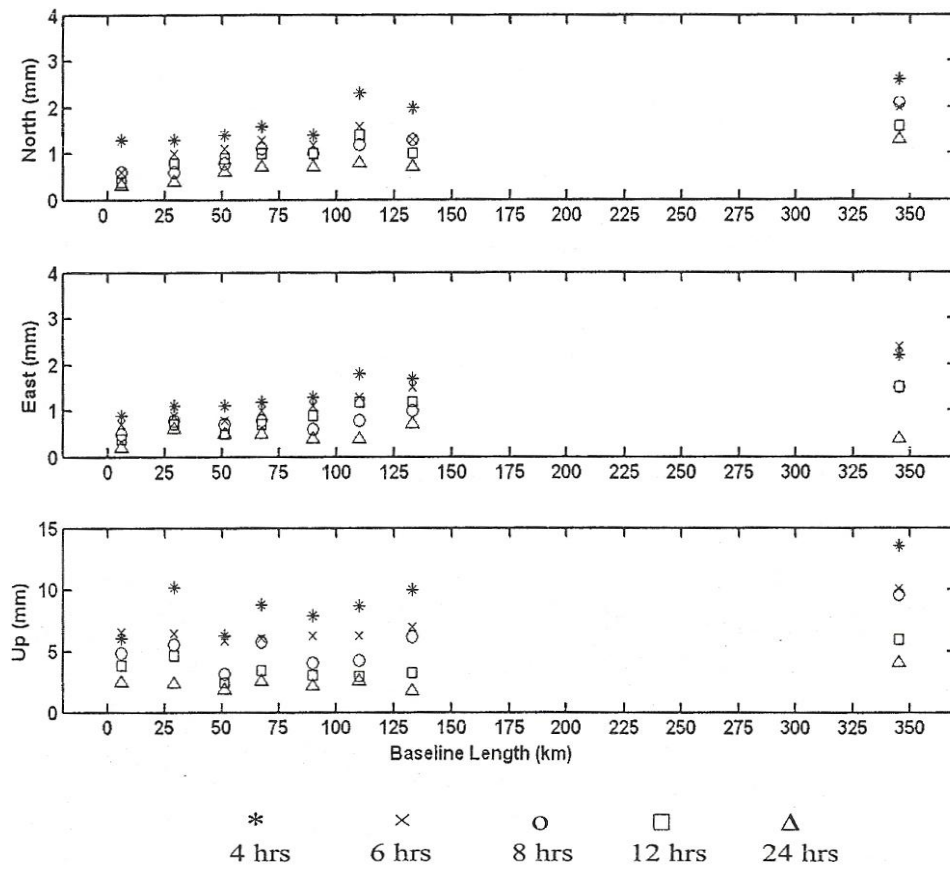


Figure 5.3. RMS values for each baseline and each value of T according to Dogan, (2007)

The results presented in the study, regarding the dependency on baseline length, agree with the ones given in Eckl *et al.*, (2001). They contradict with the ones derived by Dogan, (2007). This could perhaps be ascribed to poor baseline sampling between 150 km and 300 km in Dogan, (2007). However empirical prediction formulas derived for shorter baselines (baselines shorter than 300 km) still show some agreement in determined confidence intervals for baselines up to 2000 km. The results that have been presented by Ozer, (2004) are not statistically suggestive due to the limited sampling that has been used.

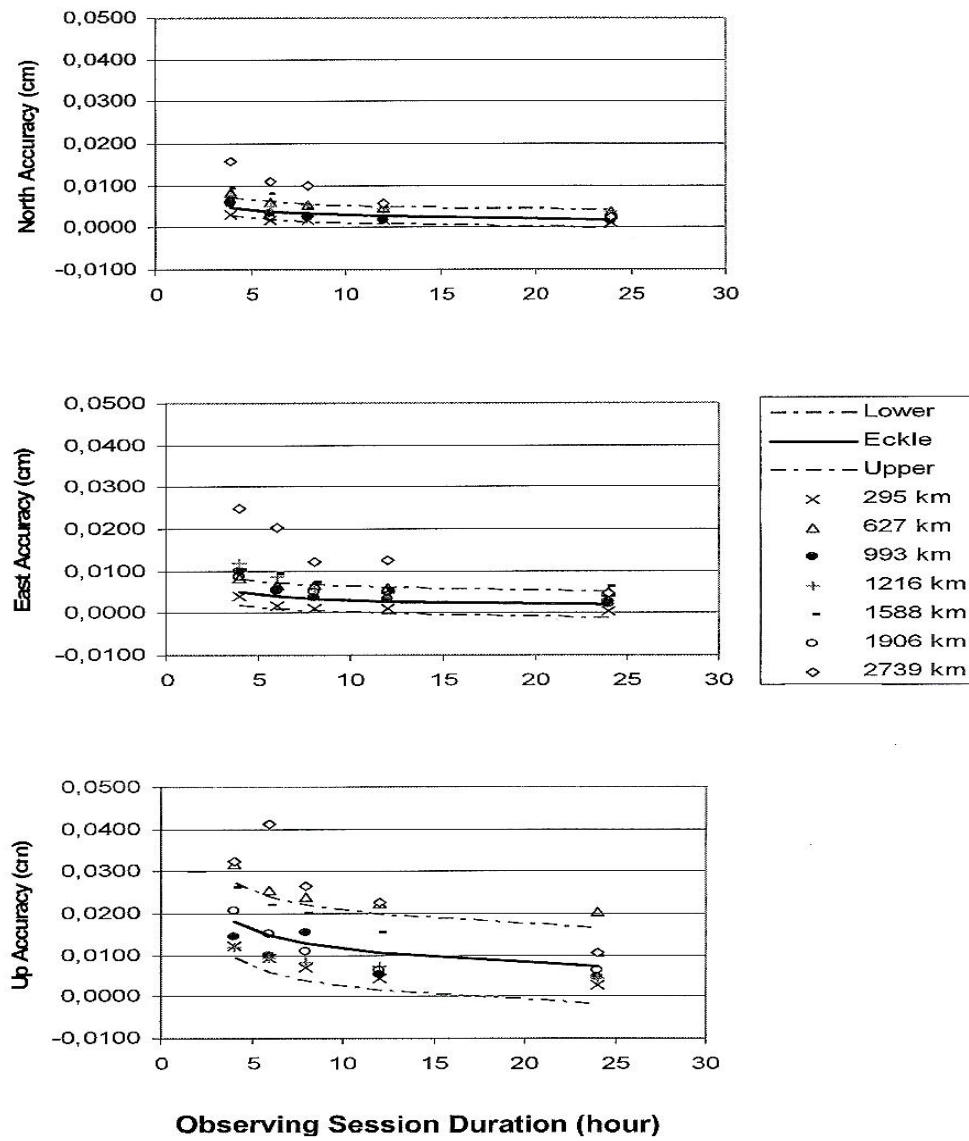


Figure 5.4. Solutions plotted against the predicted curve by Eckle *et al.*, (2001).

Upper and lower bounds of the prediction are given with the dashed lines

(Engin and Sanli, 2009)

6. PREPERATION AND PROCESSING THE GPS DATA

GPS data used in this study have been obtained from SOPAC (Scripps Orbit and Permanent Array Center) archives and the stations are chosen from EUREF (European Reference Frame) and IGS network. The permanent GPS stations used in the study are shown in Figure 6.1 below. GPS data is obtained in Receiver Independent Exchange (RINEX) format and sampled with 15° elevation cut off angle and 30 second recording intervals. As mentioned previously, JPL's GIPSY/OASIS II software was used to process the GPS data. Baseline components were determined by fixing the ambiguities and using the PPP (Precise Point Positioning) algorithm, which was developed by Zumberge *et al.*, (1997). Ocean tide loading effect was eliminated by using Schernek's model (<http://www.oso.chalmers.se/~loading/>). Carrier phase ambiguities were resolved using the technique of Blewitt, (1989). Tropospheric zenith delay was estimated stochastically by random walk model. The GPS/GIPSY PPP solutions were produced in ITRF 2000.

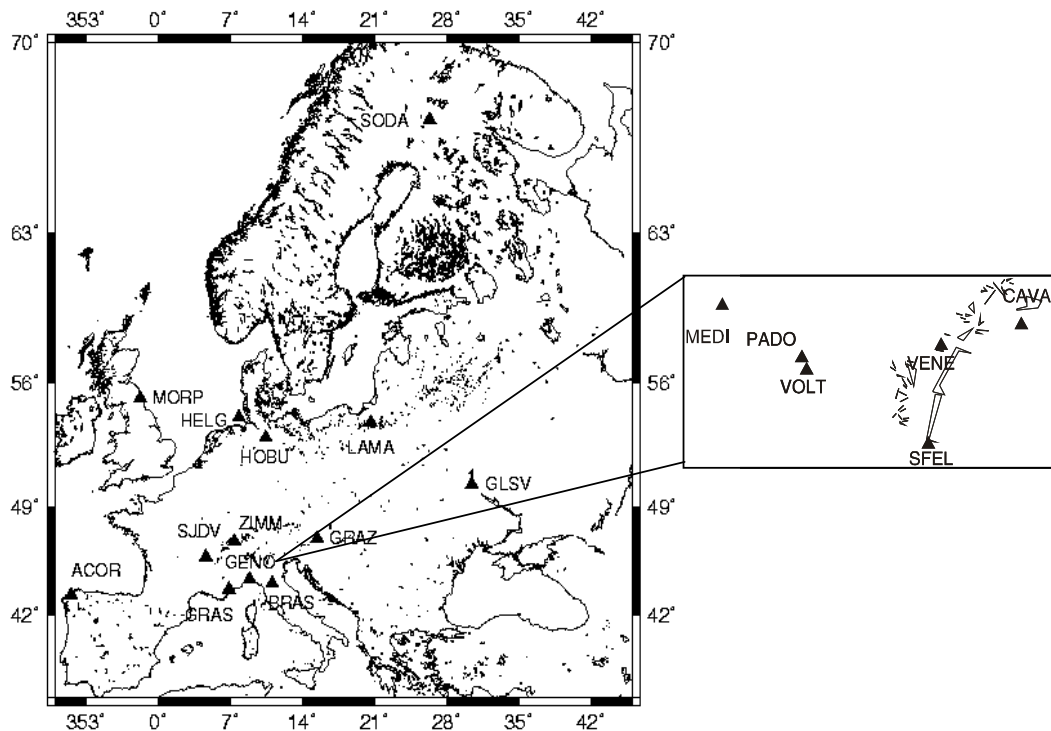


Figure 6.1. Permanent GPS stations used in the study

7. APPLICATION

7.1. Aim Of The Application

In this study our goal was to assess GPS accuracies over a baseline length which covers both short and long baselines and to try to fit a uniform model to all data used. Generally, the dependency of observing session duration and baseline length on the GPS accuracy is examined. The stations were chosen homogeneously from IGS points and we paid attention not to take the stations located on a straight line. We tried to choose the points from all directions and we used data that was almost evenly sampled to increase the reliability of our results.

7.2. Computing Rms Values

Baseline lengths were ranging from 3 to 3000 km. GPS stations were chosen from IGS network and EUREF stations which basically located in the continent Europe. GPS data were downloaded from SOPAC archives for the baselines formed. The names of the 13 baselines are given respectively in Table 7.2.1.

Table 7.2.1. Names and the lengths of the baselines used in the study

Baseline	Length (km)
PADO-VOLT	3
SFEL-VEVE	23
VOLT-VEVE	33
SFEL-MEDI	93
BRAS-VOLT	153
CAVA-HFLK	223
SJDV-GRAS	295
MORP-HELG	627
HOBV-BRAS	993
LAMA-ZIMM	1216
HELG-GLSV	1588
ACOR-GRAZ	1906
SODA-GENO	2739

For each baseline, 10 days of GPS data observed in January 2005 were selected and each day's data were subdivided into 6, 8 and 12 hours observing sessions. Minimum observing session was taken to be 6 hours considering long baseline processing requires session lengths longer than 4-hour (Engin and Sanli, 2009). For each subset of data, the positional coordinates were computed by using PPP method. When using the PPP routine, the ambiguities are not fixed. Not fixing the ambiguities does not cause problems with vertical positioning. By fixing ambiguities, the accuracy of the horizontal positioning can be improved by about 2-4 mm (Blewitt, 2008). In our research, the carrier phase ambiguities were resolved using the technique discussed in Blewitt, (1989). Having fixed the ambiguities PPP results can be easily converted to north, east, and up values using GIPSY routines. For each day and each unknown point, a position was computed for each 24 hour session. The average position from the ten 24 h sessions was then adopted as the true position of the point. For each baseline, the differences in north, east and up from this true position were determined for every observing session as described in Soler *et al.*, (2005) but using GIPSY utilities. The RMS values are then calculated by using these differences. The RMS of a collection of n values is given by the formula:

$$x_{rms} = \sqrt{\frac{1}{n} \sum_{i=1}^n x_i^2} = \sqrt{\frac{x_1^2 + x_2^2 + \dots x_n^2}{n}} \quad (7.1)$$

Here n is the number of observations made during the subdivided sessions and x values are the differences taken from 24-hour sessions.

The 24-hour data is chosen as the true value, because during 24 hours all the satellite configurations are studied and errors caused due to the satellite receiver geometry and multipath are mainly eliminated.

The calculated RMS values in each component, for each baseline and for each value of T are given as a chart by Table 7.2.2. It is obviously seen that the RMS values in the up direction is larger than that in the horizontal components (north or east).

Table 7.2.2. RMS values (mm) of north, east and up for each baseline and each value of T

		3 km	23 km	33 km	93 km	153 km	223 km	295 km
6h	RMS n (mm)	1.8	2.2	2.0	2.2	3.1	3.4	1.9
	RMS e (mm)	1.7	1.3	1.6	2.5	1.9	2.7	1.6
	RMS u (mm)	7.9	5.0	6.3	5.6	8.2	8.6	9.3
8h	RMS n (mm)	1.6	1.7	1.7	1.8	2.5	2.6	1.9
	RMS e (mm)	1.3	0.9	1.1	2.3	1.5	2.6	1.2
	RMS u (mm)	6.2	4.6	4.9	6.8	5.9	6.7	6.9
12h	RMS n (mm)	1.0	1.3	1.6	1.3	2.3	1.9	1.7
	RMS e (mm)	1.1	0.9	1.0	2.2	1.3	2.0	1.1
	RMS u (mm)	5.9	3.1	5.2	4.3	5.5	5.2	4.3
24h	RMS n (mm)	0.7	1.0	0.8	1.0	1.5	1.8	1.0
	RMS e (mm)	0.9	0.5	0.7	2.0	1.0	1.7	0.5
	RMS u (mm)	3.8	2.4	3.9	3.8	4.3	1.2	2.6
		627 km	993 km	1216 km	1588 km	1906 km	2739 km	
6h	RMS n (mm)	6.0	3.5	4.9	8.0	2.3	11.0	
	RMS e (mm)	6.6	5.5	8.6	9.3	5.4	20.2	
	RMS u (mm)	25.4	10.0	9.2	22.0	15.0	41.2	
8h	RMS n (mm)	5.2	2.4	5.2	4.4	2.7	9.8	
	RMS e (mm)	6.6	3.7	5.7	7.4	5.0	12.2	
	RMS u (mm)	23.8	15.5	8.2	19.9	11.0	26.6	
12h	RMS n (mm)	4.7	1.8	4.2	4.6	1.8	5.6	
	RMS e (mm)	6.0	3.4	4.7	5.3	5.0	12.6	
	RMS u (mm)	22.3	5.4	7.2	15.4	6.2	22.7	
24h	RMS n (mm)	3.7	1.5	3.6	3.0	1.6	2.3	
	RMS e (mm)	4.9	2.6	4.2	6.2	2.2	4.8	
	RMS u (mm)	20.4	4.8	4.4	9.7	6.4	10.4	

Graphics for each baseline are drawn in all directions and they show the relationship between the session duration and the RMS values. In every direction for all of the baselines, the RMS values are inversely proportional with the observing session duration. To clarify this we can say that the RMS values become smaller while the observing session duration gets larger.

Table 7.2.3. Root mean square values (mm) of each baseline for north direction

PADO-VOLT	3 km	SFEL-VEVE	23 km	VOLT-VEVE	33 km
6 h	1.8	6 h	2.2	6 h	2.0
8 h	1.6	8 h	1.7	8 h	1.7
12 h	1.0	12 h	1.3	12 h	1.6
24 h	0.7	24 h	1.0	24 h	0.8
SFEL-MEDI	93 km	BRAS-VOLT	153 km	CAVA-HFLK	223 km
6 h	2.2	6 h	3.1	6 h	3.4
8 h	1.8	8 h	2.5	8 h	2.6
12 h	1.3	12 h	2.3	12 h	1.9
24 h	1.0	24 h	1.5	24 h	1.8
SJDV-GRAS	295 km	MORP-HELG	627 km	HOBV-BRAS	993 km
6 h	1.9	6 h	6.0	6 h	3.5
8 h	1.9	8 h	5.2	8 h	2.4
12 h	1.7	12 h	4.7	12 h	1.8
24 h	1.0	24 h	3.7	24 h	1.5
LAMA-ZIMM	1216 km	HELG-GLSV	1588 km	ACOR-GRAZ	1906 km
6 h	4.9	6 h	8.0	6 h	2.3
8 h	5.2	8 h	4.4	8 h	2.7
12 h	4.2	12 h	4.6	12 h	1.8
24 h	3.6	24 h	3.0	24 h	1.6
SODA-GENO	2739 km				
6 h	11.0				
8 h	9.8				
12 h	5.6				
24 h	2.3				

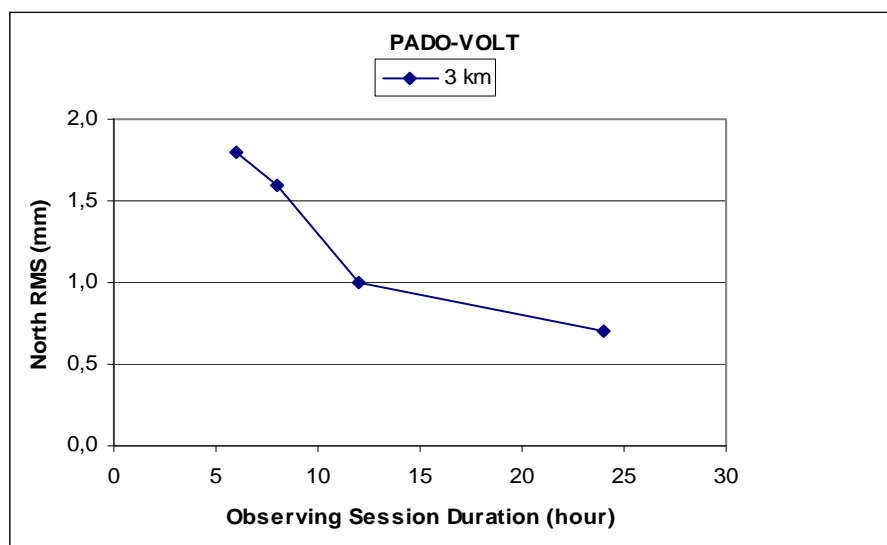


Figure 7.2.1. RMS values of north direction for the PADO-VOLT baseline

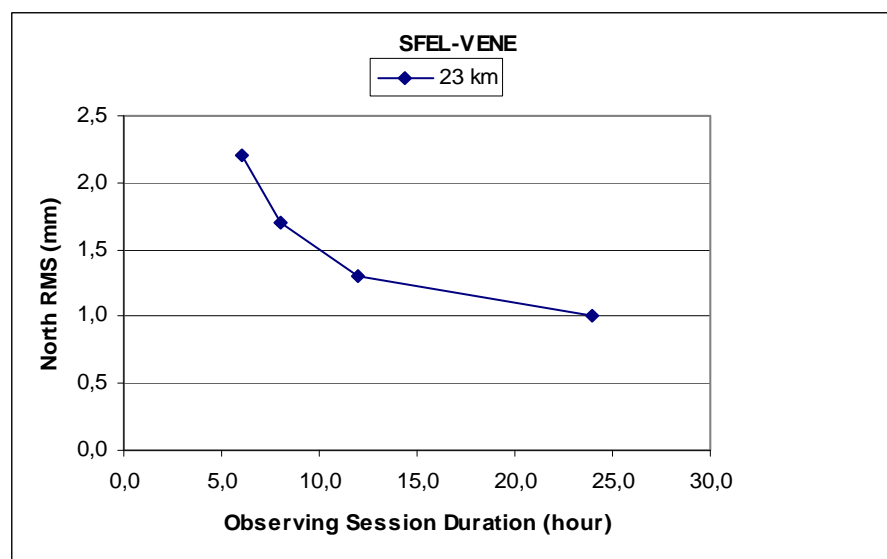


Figure 7.2.2. RMS values of north direction for the SFEL-VENE baseline

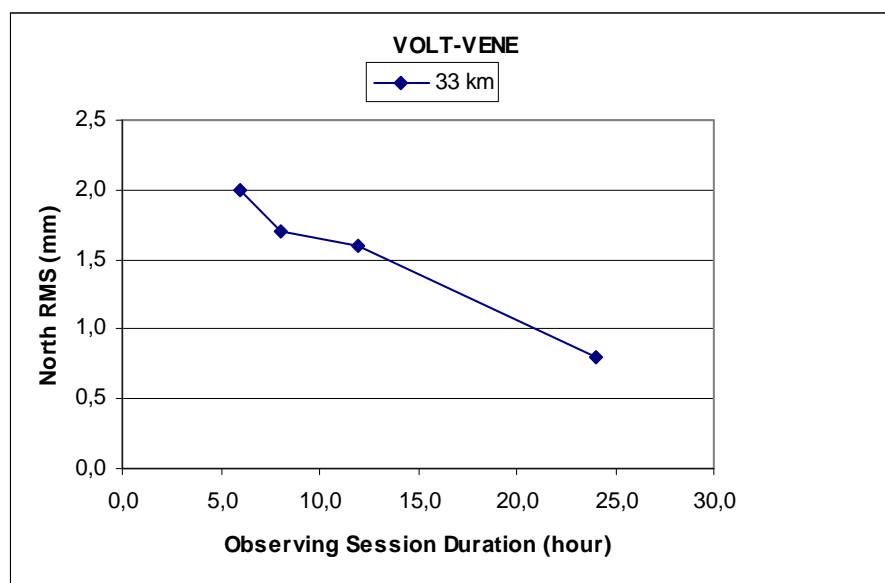


Figure 7.2.3. RMS values of north direction for the VOLT-VE NE baseline

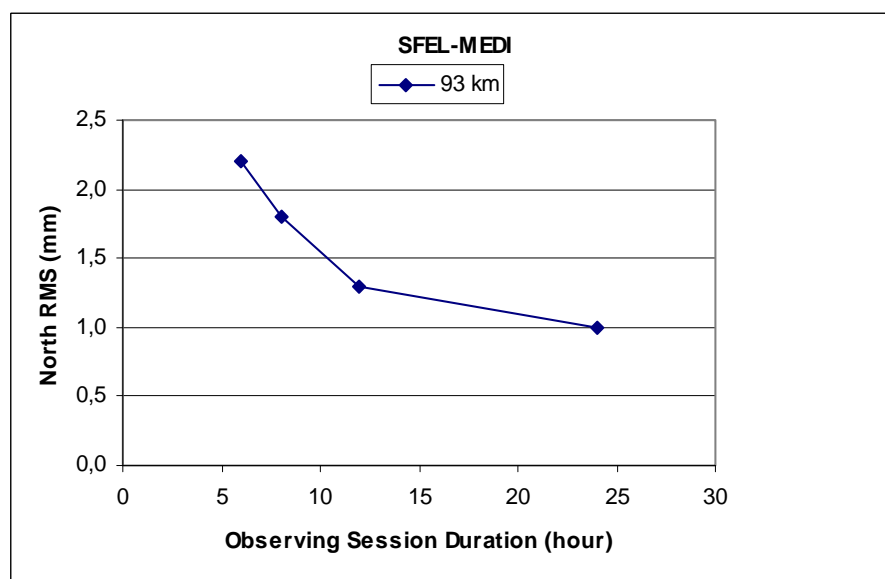


Figure 7.2.4. RMS values of north direction for the SFEL-MEDI baseline

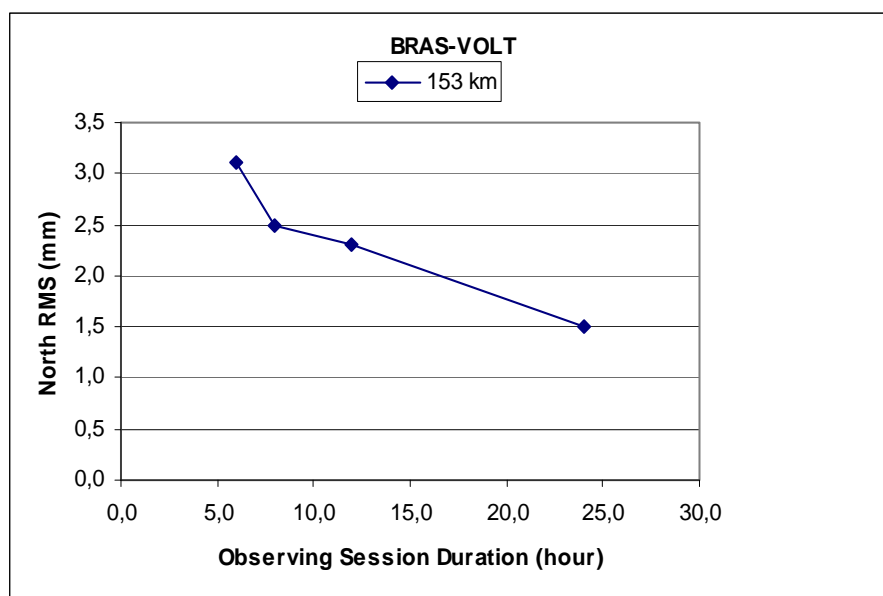


Figure 7.2.5. RMS values of north direction for the BRAS-VOLT baseline

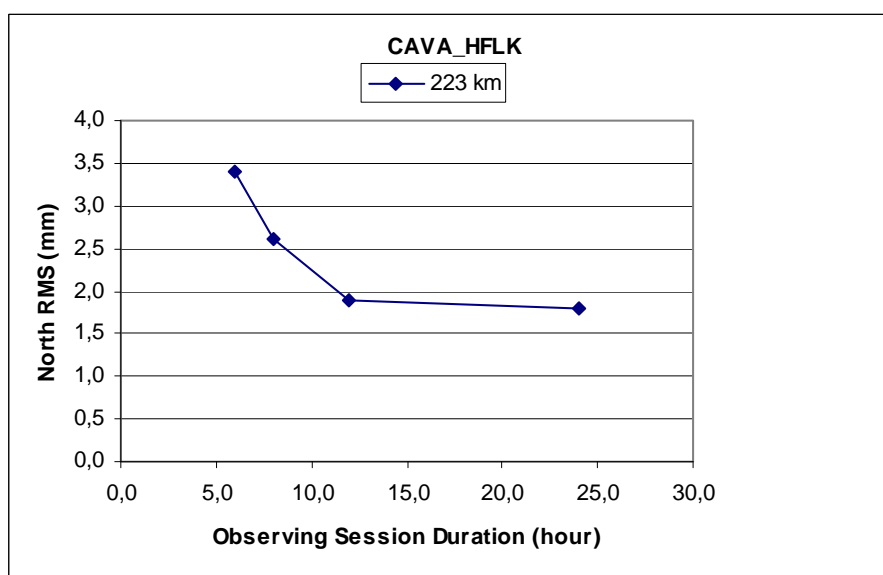


Figure 7.2.6. RMS values of north direction for the CAVA-HFLK baseline

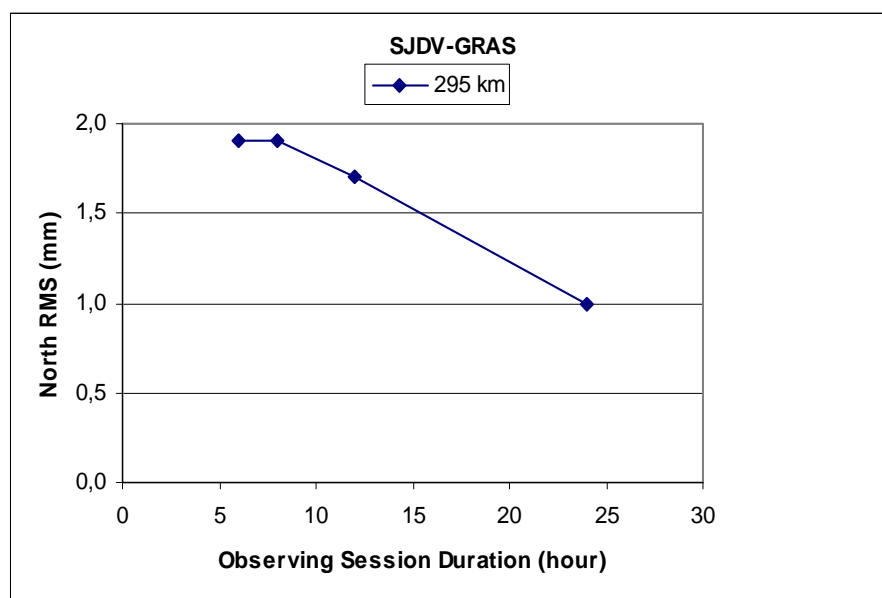


Figure 7.2.7. RMS values of north direction for the SJDV-GRAS baseline

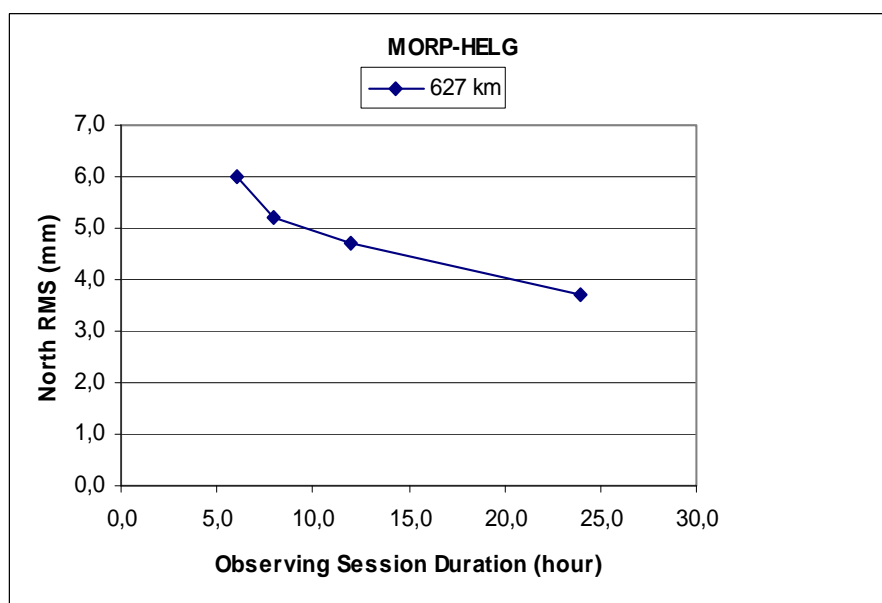


Figure 7.2.8. RMS values of north direction for the MORP-HELG baseline

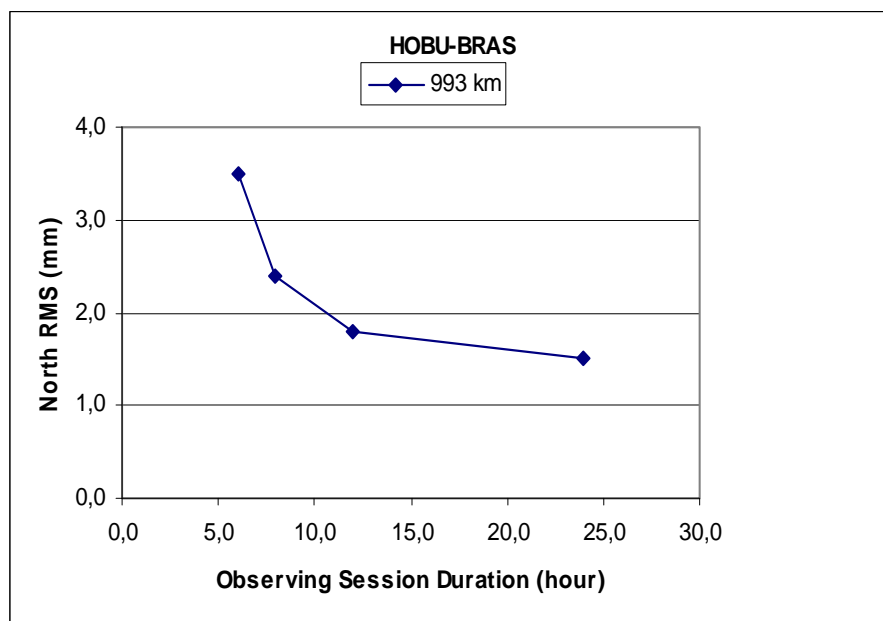


Figure 7.2.9. RMS values of north direction for the HOB-UBRAS baseline

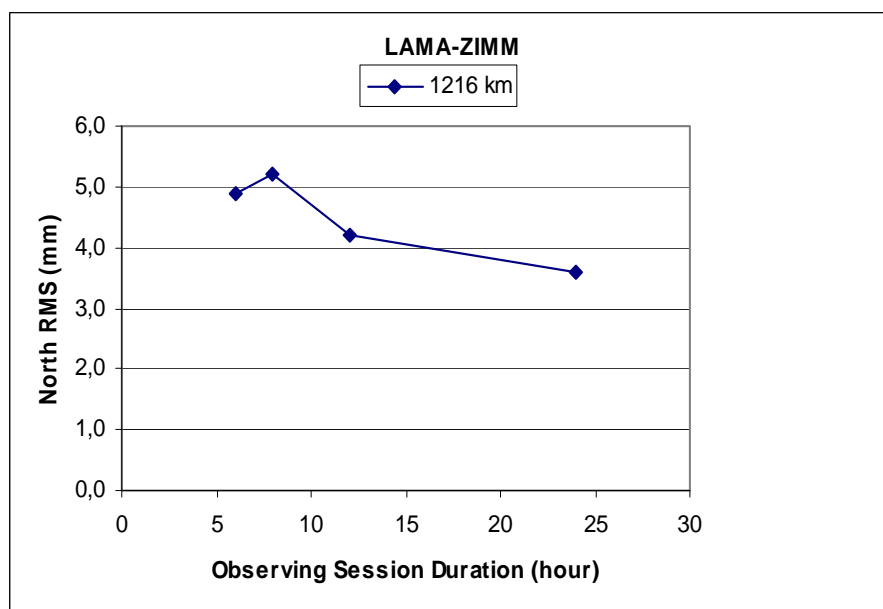


Figure 7.2.10. RMS values of north direction for the LAMA-ZIMM baseline

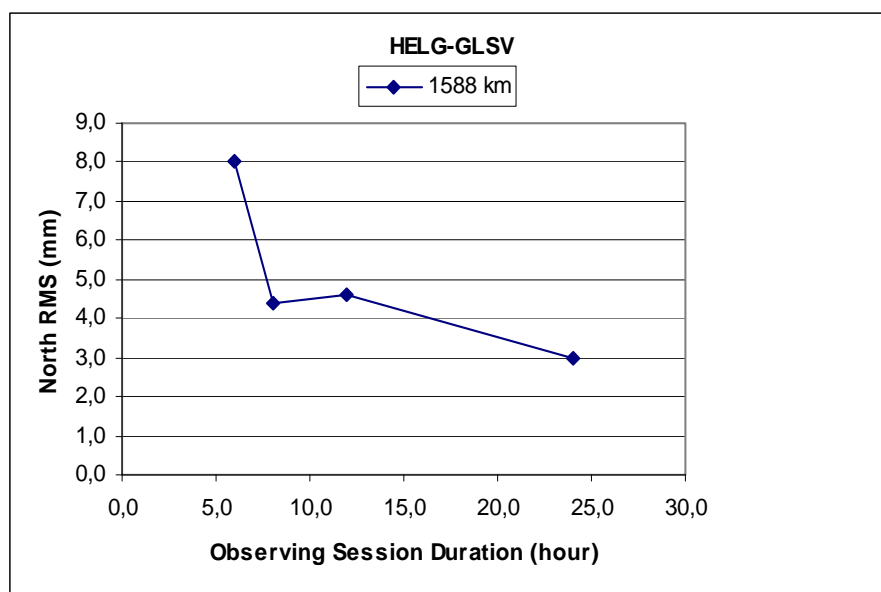


Figure 7.2.11. RMS values of north direction for the HELG-GLSV baseline

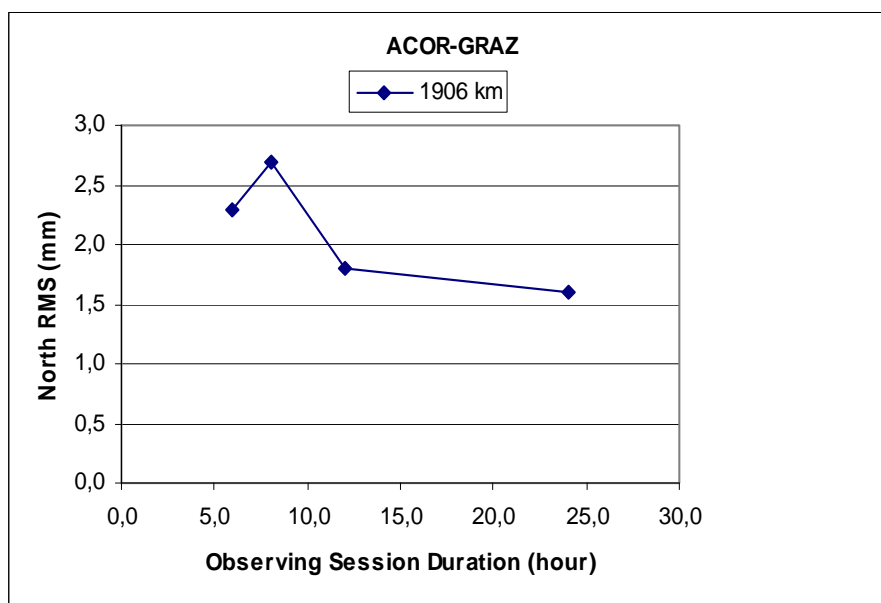


Figure 7.2.12. RMS values of north direction for the ACOR-GRAZ baseline

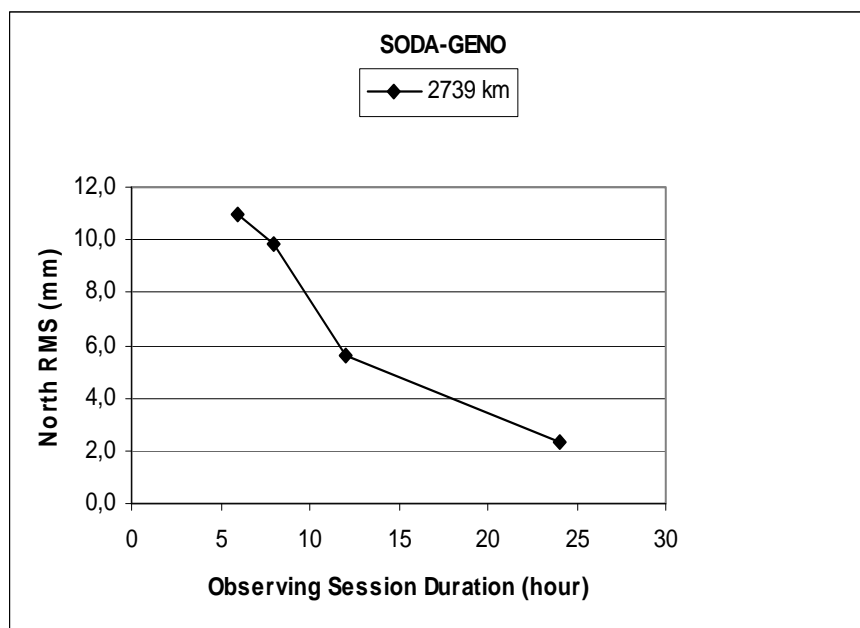


Figure 7.2.13. RMS values of north direction for the SODA-GENO baseline

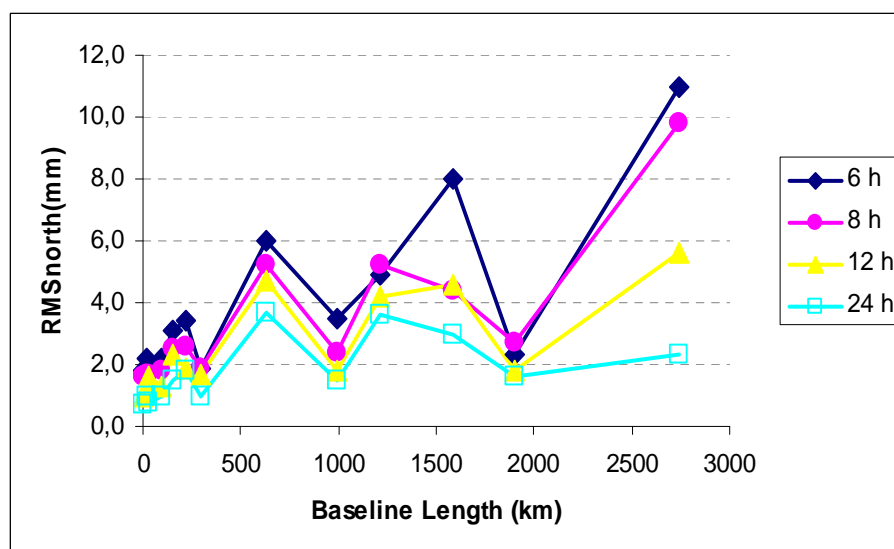


Figure 7.2.14. Relationship between RMS values of north direction, baseline length and T

Table 7.2.4. Root mean square values (mm) of each baseline for east direction

PADO-VOLT	3 km	SFEL-VE NE	23 km	VOLT-VE NE	33 km
6 h	1.7	6 h	1.3	6 h	1.6
8 h	1.3	8 h	0.9	8 h	1.1
12 h	1.1	12 h	0.9	12 h	1.0
24 h	0.9	24 h	0.5	24 h	0.7
SFEL-MEDI	93 km	BRAS-VOLT	153 km	CAVA-HFLK	223 km
6 h	2.5	6 h	1.9	6 h	2.7
8 h	2.3	8 h	1.5	8 h	2.6
12 h	2.2	12 h	1.3	12 h	2.0
24 h	2.0	24 h	1.0	24 h	1.7
SJDV-GRAS	295 km	MORP-HEL G	627 km	HOB U-BRAS	993 km
6 h	1.6	6 h	6.6	6 h	5.5
8 h	1.2	8 h	6.6	8 h	3.7
12 h	1.1	12 h	6.0	12 h	3.4
24 h	0.5	24 h	4.9	24 h	2.6
LAMA-ZIMM	1216 km	HEL G-GLSV	1588 km	ACOR-GRAZ	1906 km
6 h	8.6	6 h	9.3	6 h	5.4
8 h	5.7	8 h	7.4	8 h	5.0
12 h	4.7	12 h	5.3	12 h	5.0
24 h	4.2	24 h	6.2	24 h	2.2
SODA-GENO	2739 km				
6 h	20.2				
8 h	12.2				
12 h	12.6				
24 h	4.8				

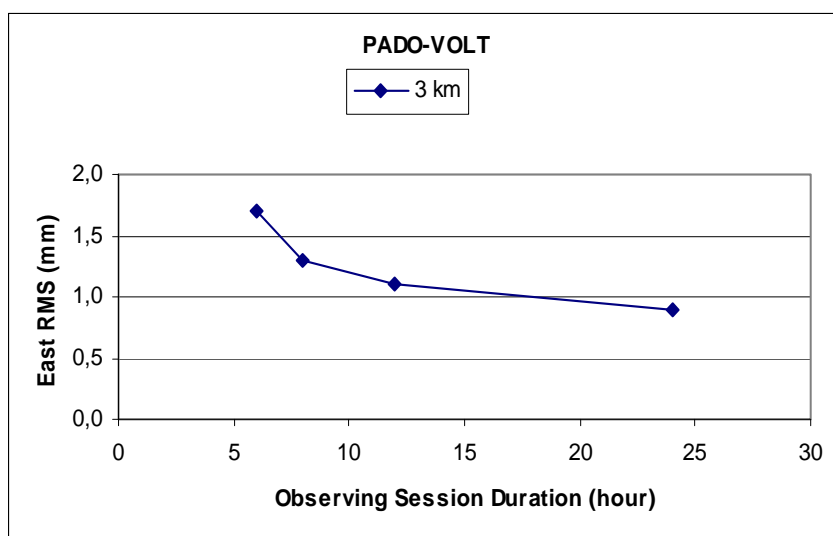


Figure 7.2.15. RMS values of east direction for the PADO-VOLT baseline

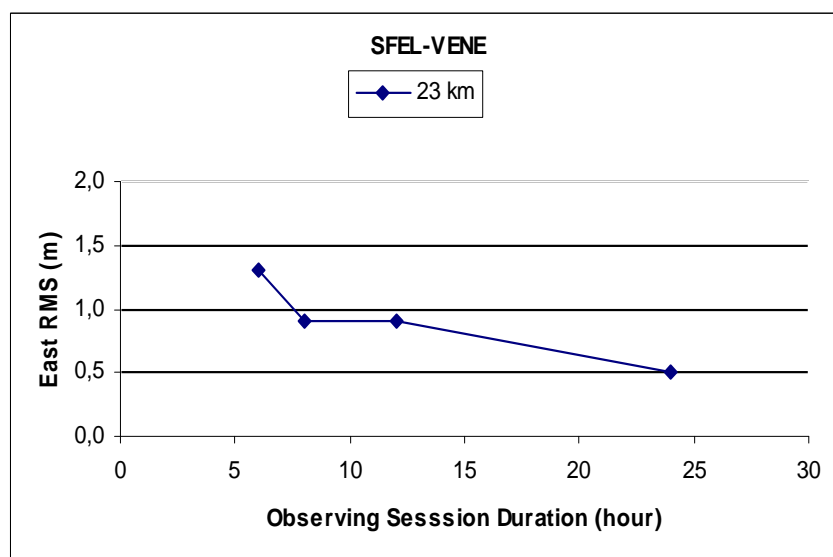


Figure 7.2.16. RMS values of east direction for the SFEL-VENE baseline

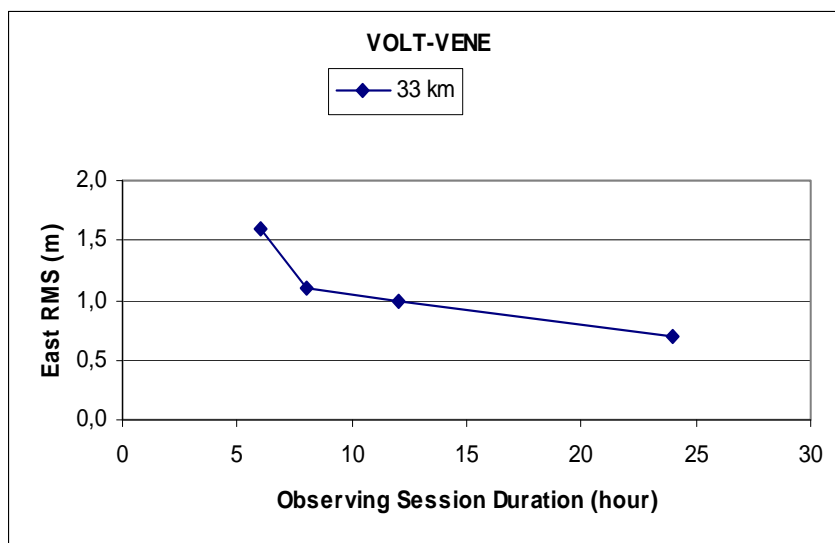


Figure 7.2.17. RMS values of east direction for the VOLT-VENE baseline

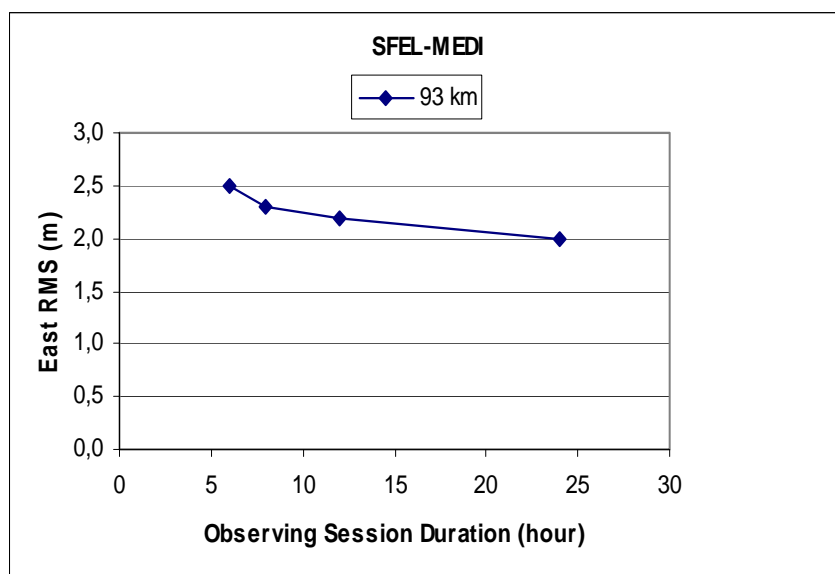


Figure 7.2.18. RMS values of east direction for the SFEL-MEDI baseline

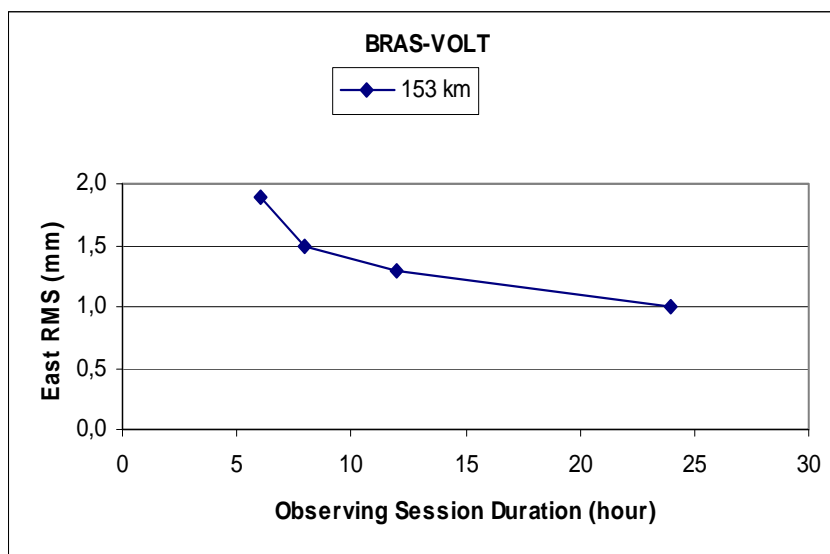


Figure 7.2.19. RMS values of east direction for the BRAS-VOLT baseline

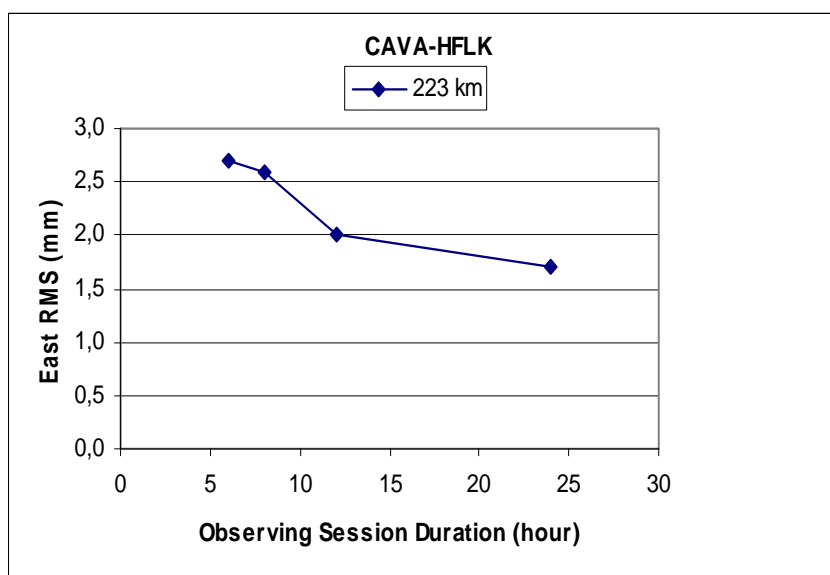


Figure 7.2.20. RMS values of east direction for the CAVA-HFLK baseline

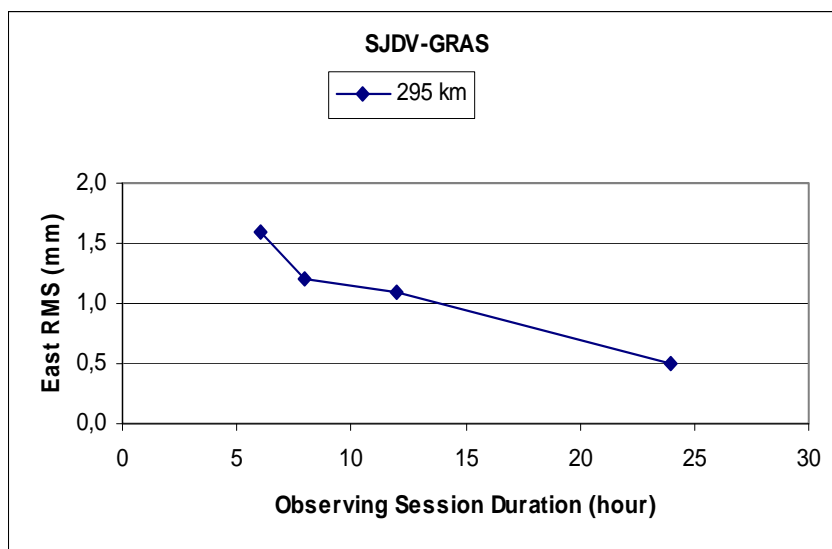


Figure 7.2.21. RMS values of east direction for the SJDV-GRAS baseline

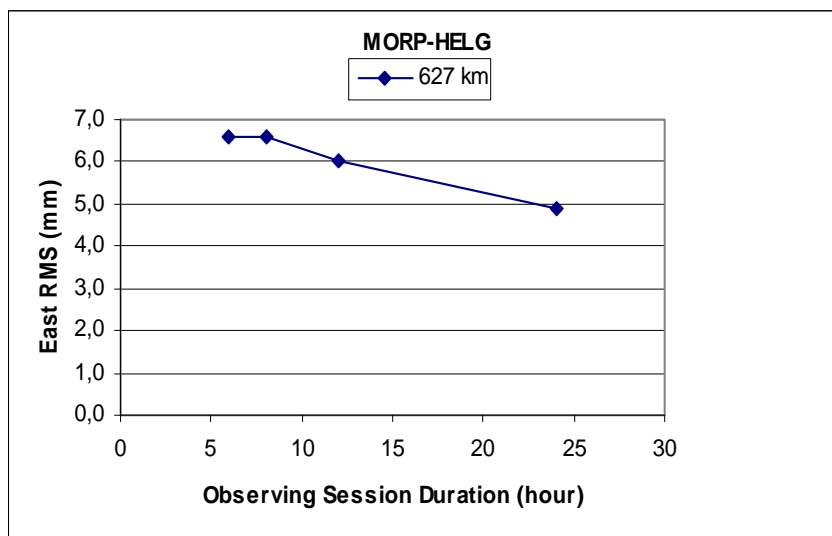


Figure 7.2.22. RMS values of east direction for the MORP-HELG baseline

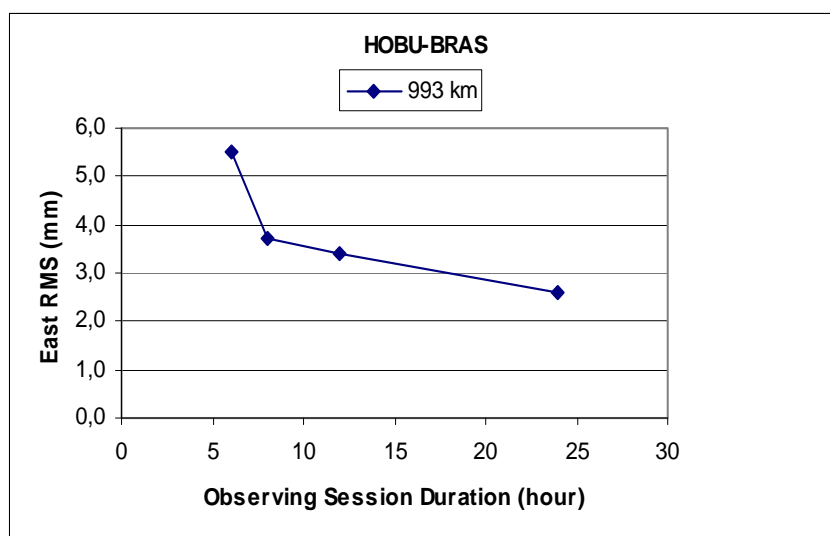


Figure 7.2.23. RMS values of east direction for the HOB-UBRAS baseline

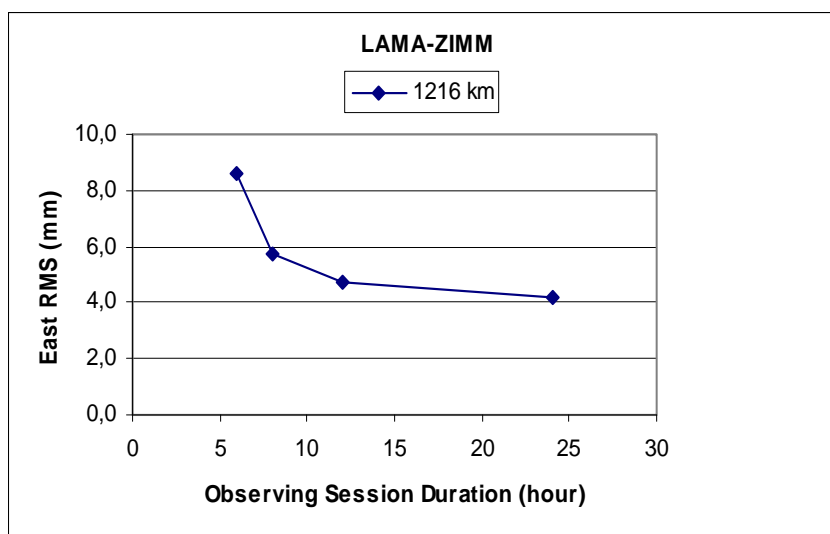


Figure 7.2.24. RMS values of east direction for the LAMA-ZIMM baseline

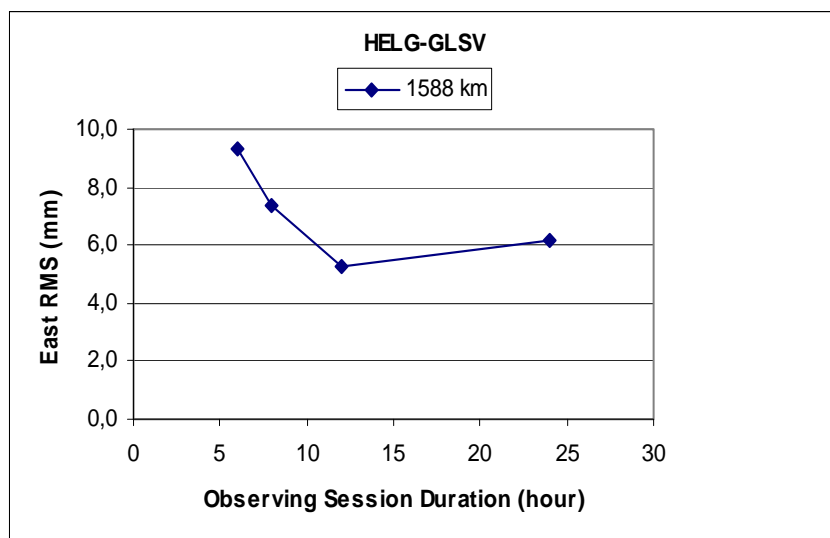


Figure 7.2.25. RMS values of east direction for the HELG-GLSV baseline

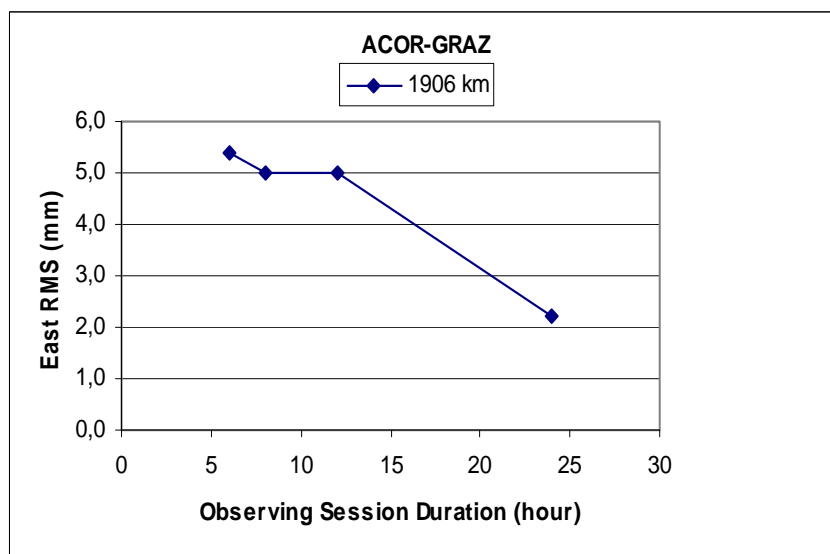


Figure 7.2.26. RMS values of east direction for the ACOR-GRAZ baseline

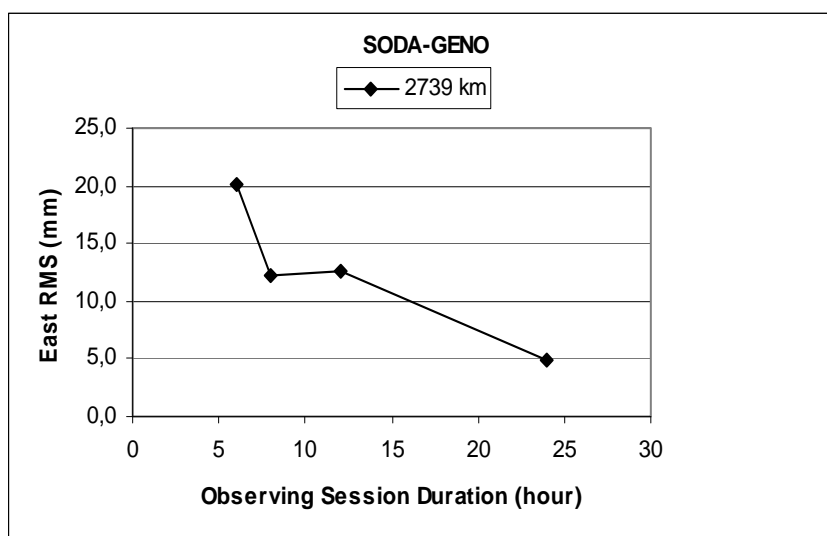


Figure 7.2.27 RMS values of east direction for the SODA-GENO baseline

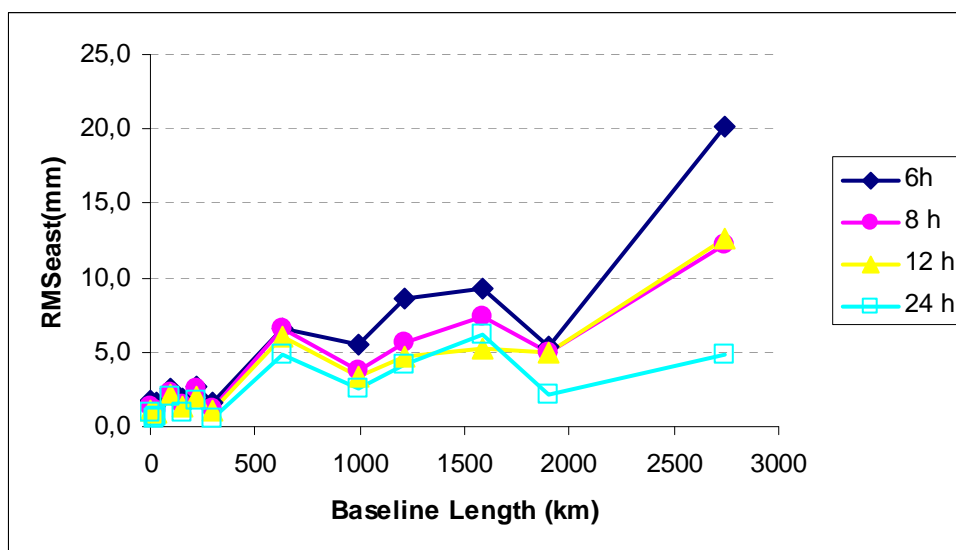


Figure 7.2.28. Relationship between RMS values of east direction, baseline length and T

Table 7.2.5. Root mean square values (mm) of each baseline for up direction

PADO-VOLT	3 km	SFEL-VE NE	23 km	VOLT-VE NE	33 km
6 h	7.9	6 h	5.0	6 h	6.3
8 h	6.2	8 h	4.6	8 h	4.9
12 h	5.9	12 h	3.1	12 h	5.2
24 h	3.8	24 h	2.4	24 h	3.9
SFEL-MEDI	93 km	BRAS-VOLT	153 km	CAVA-HFLK	223 km
6 h	5.6	6 h	8.2	6 h	8.6
8 h	6.8	8 h	5.9	8 h	6.7
12 h	4.3	12 h	5.5	12 h	5.2
24 h	3.8	24 h	4.3	24 h	1.2
SJDV-GRAS	295 km	MORP-HEL G	627 km	HOB U-BRAS	993 km
6 h	9.3	6 h	25.4	6 h	10.0
8 h	6.9	8 h	23.8	8 h	15.5
12 h	4.3	12 h	22.3	12 h	5.4
24 h	2.6	24 h	20.4	24 h	4.8
LAMA-ZIMM	1216 km	HEL G-GLSV	1588 km	ACOR-GRAZ	1906 km
6 h	9.2	6 h	22.0	6 h	15.0
8 h	8.2	8 h	19.9	8 h	11.0
12 h	7.2	12 h	15.4	12 h	6.2
24 h	4.4	24 h	9.7	24 h	6.4
SODA-GENO	2739 km				
6 h	41.2				
8 h	26.6				
12 h	22.7				
24 h	10.4				

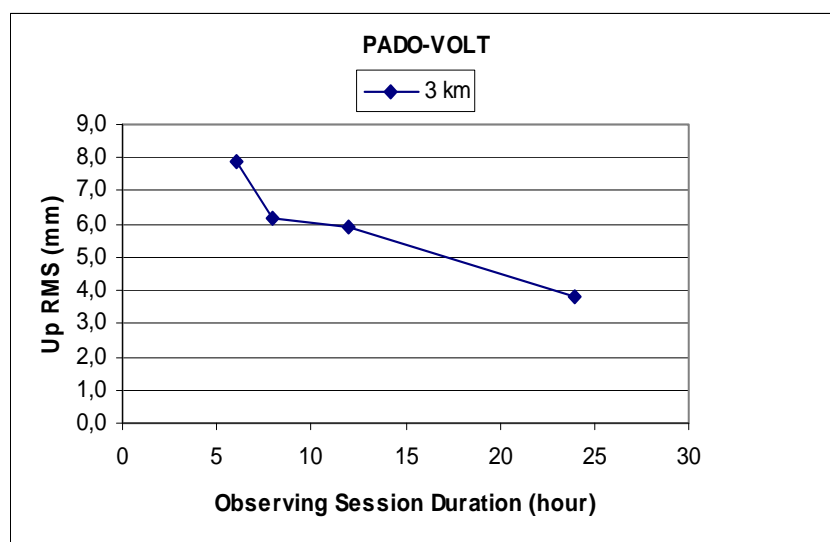


Figure 7.2.29. RMS values of up direction for the PADO-VOLT baseline

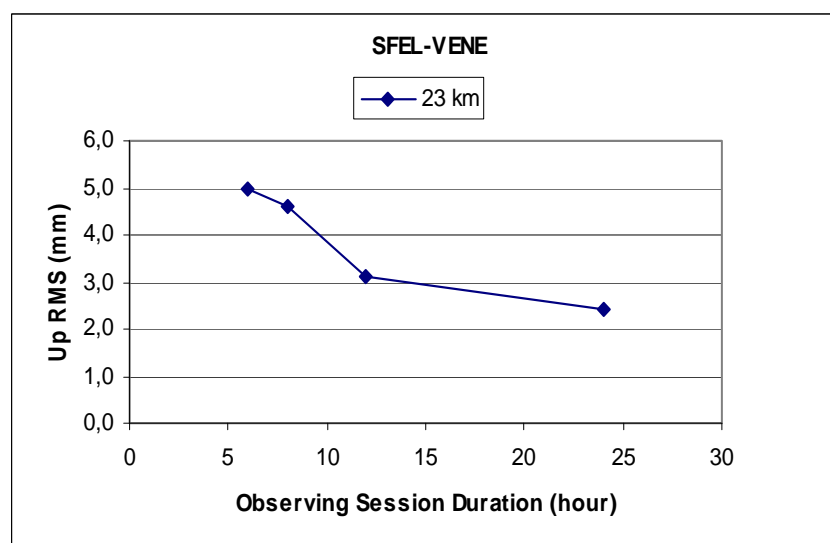


Figure 7.2.30. RMS values of up direction for the SFEL-VENE baseline

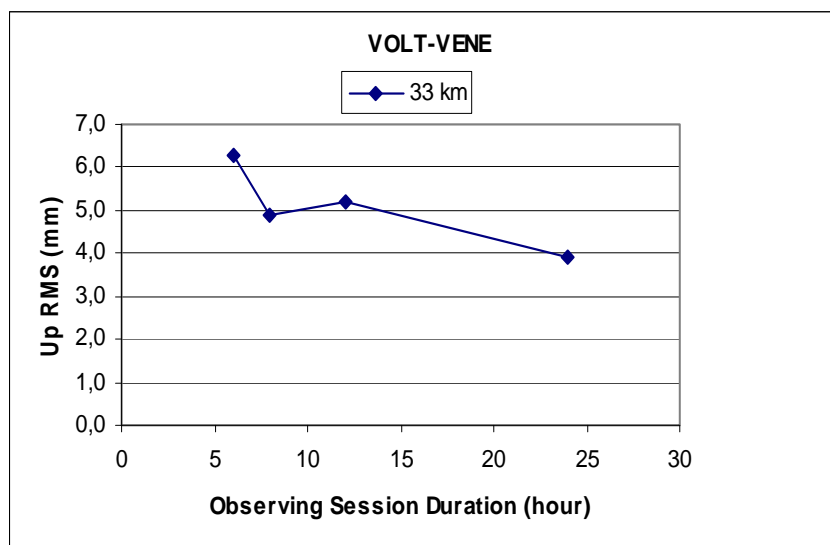


Figure 7.2.31. RMS values of up direction for the VOLT-VEVE baseline

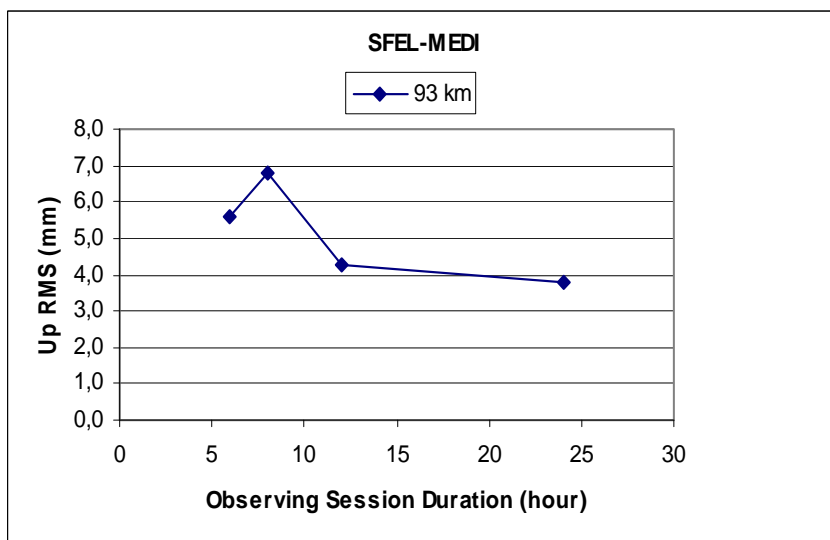


Figure 7.2.32. RMS values of up direction for the SFEL-MEDI baseline

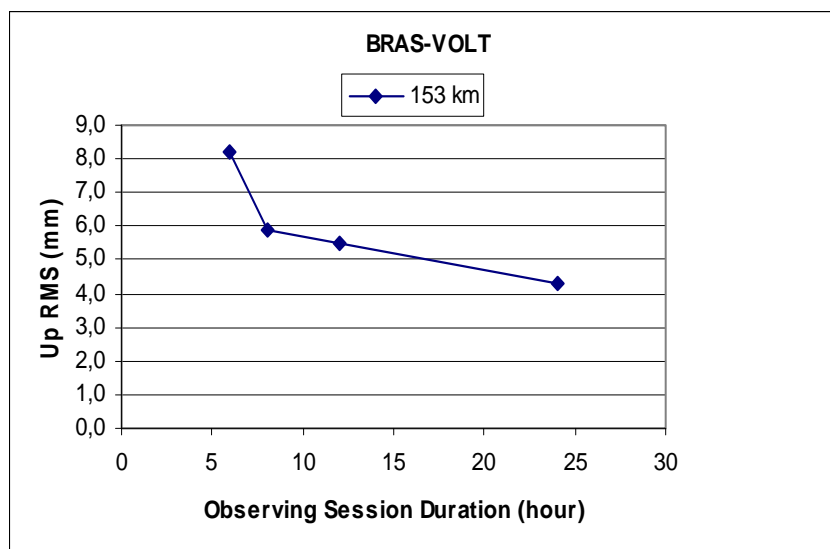


Figure 7.2.33. RMS values of up direction for the BRAS-VOLT baseline

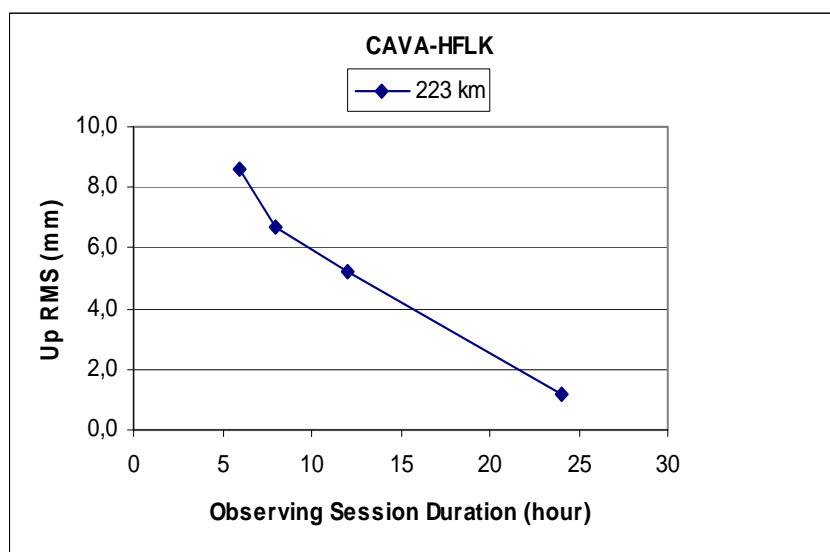


Figure 7.2.34. RMS values of up direction for the CAVA-HFLK baseline

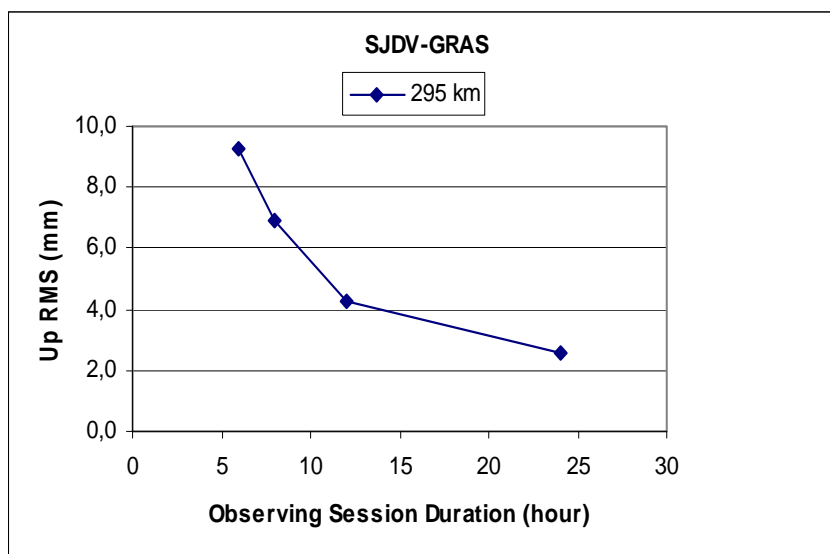


Figure 7.2.35. RMS values of up direction for the SJDV-GRAS baseline

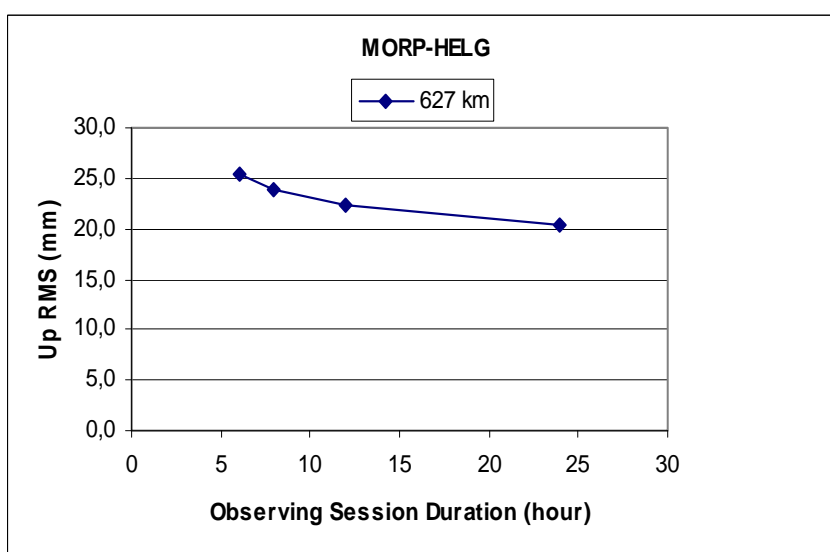


Figure 7.2.36. RMS values of up direction for the MORP-HELG baseline

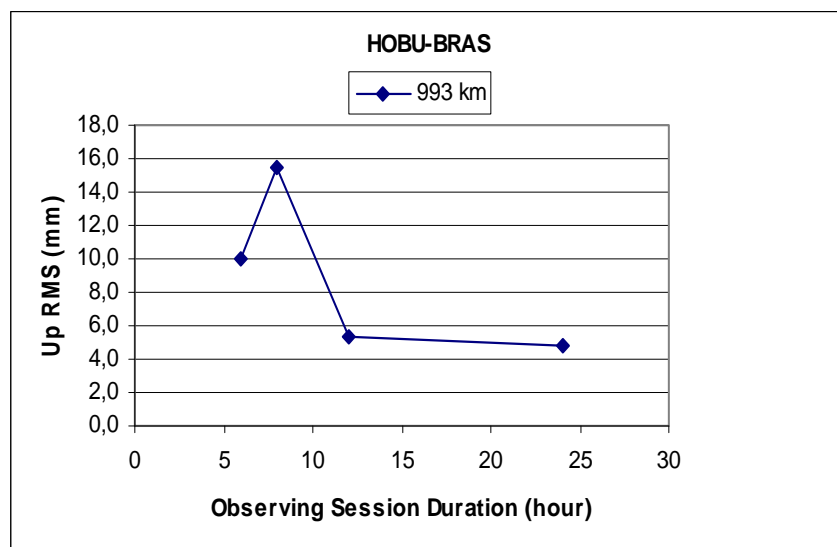


Figure 7.2.37. RMS values of up direction for the HOBUS-BRAS baseline

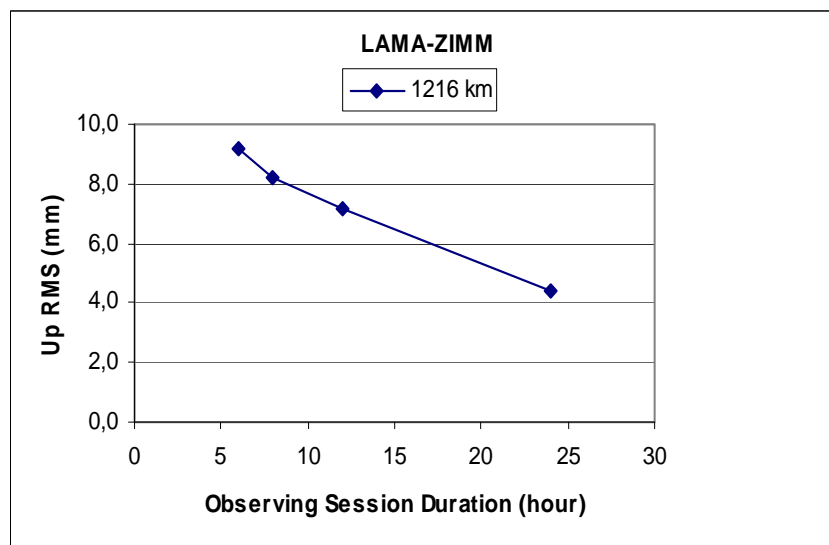


Figure 7.2.38. RMS values of up direction for the LAMA-ZIMM baseline

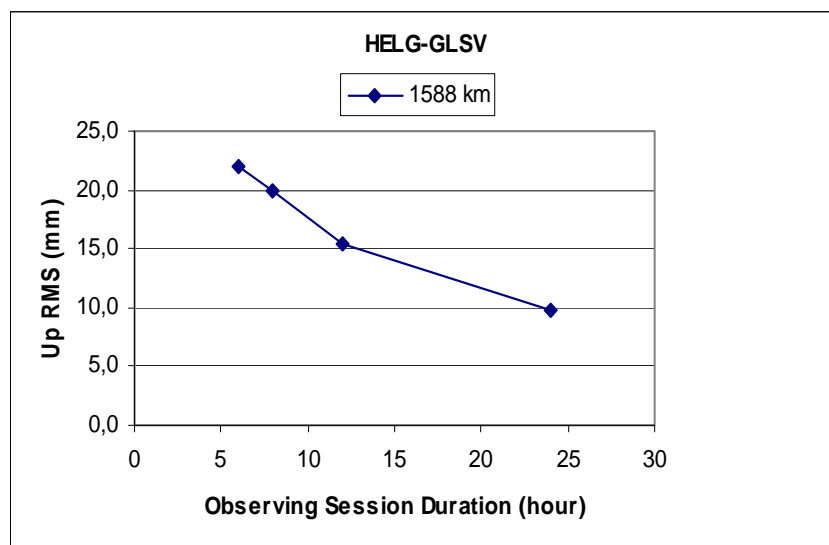


Figure 7.2.39. RMS values of up direction for the HELG-GLSV baseline

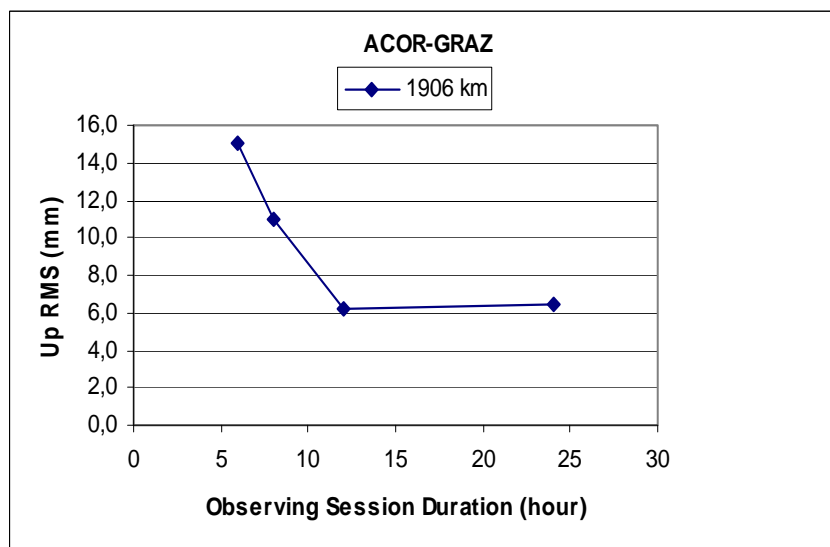


Figure 7.2.40. RMS values of up direction for the ACOR-GRAZ baseline

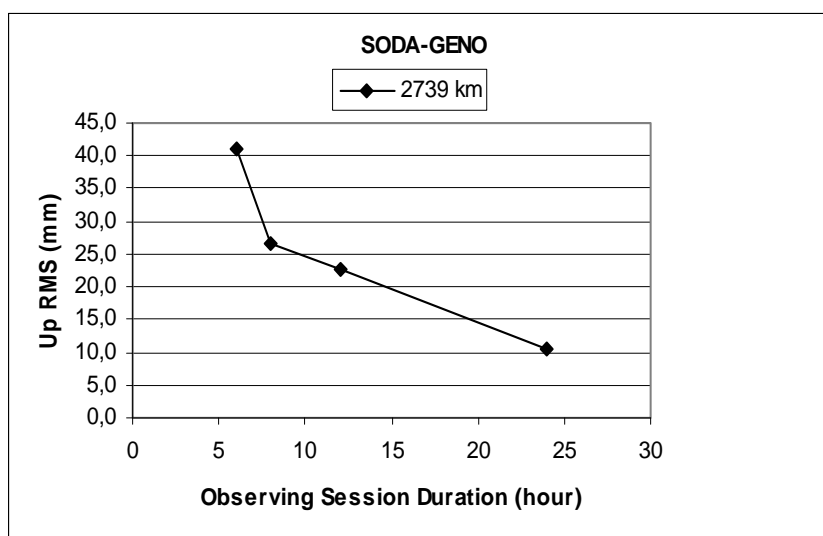


Figure 7.2.41. RMS values of up direction for the SODA-GENO baseline

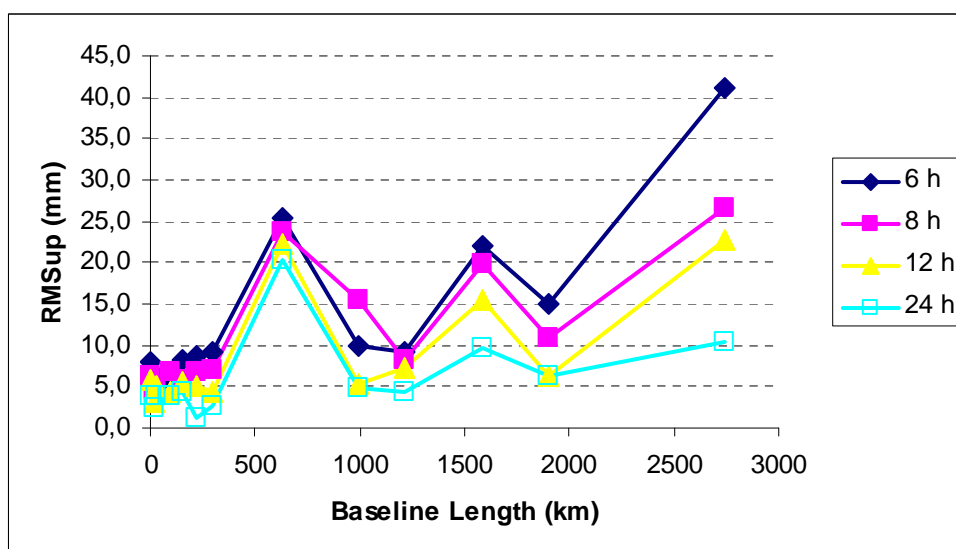


Figure 7.2.42. Relationship between RMS values of east direction, baseline length and observing session duration (T)

7.3. Least Squares Estimation

We used the functional Least Squares model which was developed by Eckl *et al.*, (2001) in order to assess GPS baselines accuracies. The following equation is used to estimate the standard error in the north-south direction, as a function of L and T .

$$S_n(L, T) = [a_n / T + b_n L^2 / T + c_n + d_n L^2]^{0.5} \quad (7.3.1)$$

Here a_n, b_n, c_n, d_n are the constants to be estimated using LS. The standard error can be represented by the square root of the sum of these four terms. As it is seen from the equation, the error terms involving a_n and b_n are inversely proportional to T , whereas those involving c_n and d_n are independent of T . The error terms involving b_n and d_n are proportional to L^2 , whereas those involving a_n and c_n are independent of L^2 (Dogan, 2007). The equations for the east-west and up-down direction are assumed by using the same form and the standard errors are computed. The estimated values of constants in Equation (7.3.1) are given in Table 7.3.2.

In Eckl *et al.*, (2001) only the constant a_n was found to be statistically significant at 95% confidence level for all GPS baseline components. Soler *et al.*, (2005) compile simplified equations from the study of Eckl *et al.*, (2001) based merely on the first term in Equation (7.3.1) According to this, the RMS errors can be computed by the equations:

$$\text{RMS (cm)} = \frac{k}{\sqrt{T}} \begin{cases} k = 1.0 \pm 0.3; \text{north / east} \\ k = 3.7 \pm 1.0; \text{vertical} \end{cases} \quad (7.3.2)$$

where T denotes the duration of the observing session expressed in hours; k is a free parameter used instead of \sqrt{a} and T is expressed in hours (Engin and Sanli, 2009).

In Engin and Sanli, (2009) the result differs from the findings of Eckl *et al.*, (2001) in that the accuracy of GPS positioning depends not only on the observing-session duration but also inter station distance. This result is somehow expected since they have worked on longer baselines. Only the coefficient b is significant according to their solutions and they finally replaced Equation (7.3.1) by

$$S_n(L, T) = [b_n L^2 / T]^{0.5} \quad (7.3.3)$$

or equivalently with similar equations for $S_e(L, T)$ and $S_u(L, T)$.

In our case by using the functional LS model given in Eckl *et al.*, (2001) we estimated new empirical constants that fit best into our solutions. According to our study, the coefficients b and d were found to be significant from LS analysis and we replaced Equation (7.3.1) by

$$S_n(L, T) = [b_n L^2 / T + d_n L^2]^{0.5} \quad (7.3.4)$$

$$S_e(L, T) = [b_e L^2 / T + d_e L^2]^{0.5} \quad (7.3.5)$$

$$S_u(L, T) = [b_u L^2 / T + d_u L^2]^{0.5} \quad (7.3.6)$$

However the function/model described with these coefficients does not fit well to the RMS of the solutions. Especially the prediction of the GPS components for 3-300 km range is affected. Hence, this does not satisfy our aim of predicting the accuracy of GPS from a unified model (*i.e.* for baselines ranging between 3 and 3000 km). Considering this, we tested alternative coefficient combinations for all three GPS baseline components north, east and up. Finally we found that for the modelling of the north and up components, the coefficients a and b are significant, whereas the east component can best be predicted by taking the coefficients a and d significant. This is illustrated in the Figures 7.3.1, 7.3.2 and 7.3.3. The mean RMS values calculated according to the alternative LSE for all components are given in Table 7.3.1.

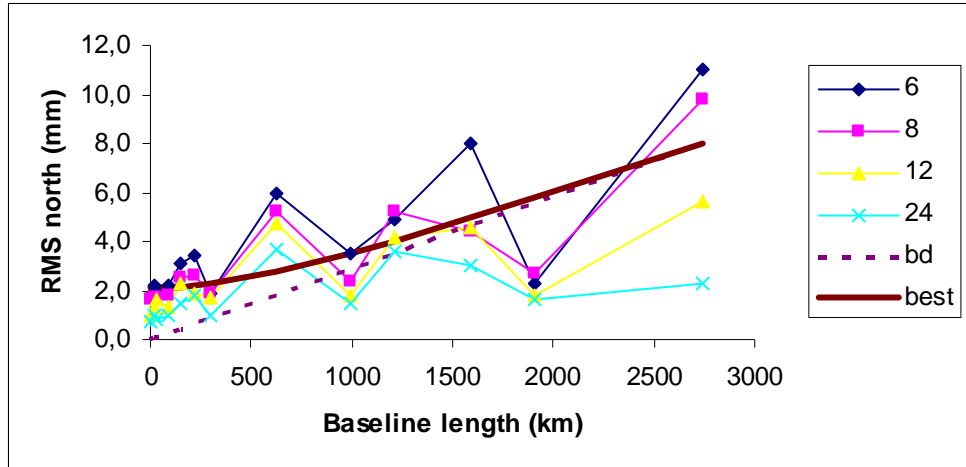


Figure 7.3.1. RMS errors and curves fit according to LSE for the north component

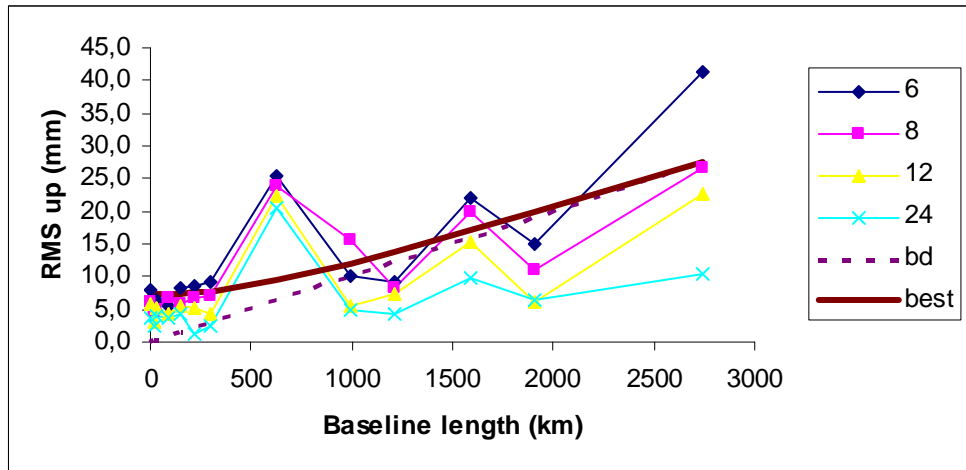


Figure 7.3.2. RMS errors and curves fit according to LSE for the up component

For north and up components Equation (7.3.1) is replaced by

$$S_n(L, T) = [a_n / T + b_n L^2 / T]^{0.5} \rightarrow S_n = \sqrt{\frac{39.3}{T} + \frac{71.96 \times 10^{-6} L^2}{T}} \quad (7.3.7)$$

$$S_u(L, T) = [a_u / T + b_u L^2 / T]^{0.5} \rightarrow S_u = \sqrt{\frac{467.846}{T} + \frac{853.57 \times 10^{-6} L^2}{T}} \quad (7.3.8)$$

where a and b are the significant coefficients for north and up components which fits best into our solutions. The results are the RMS values, expressed in mm.

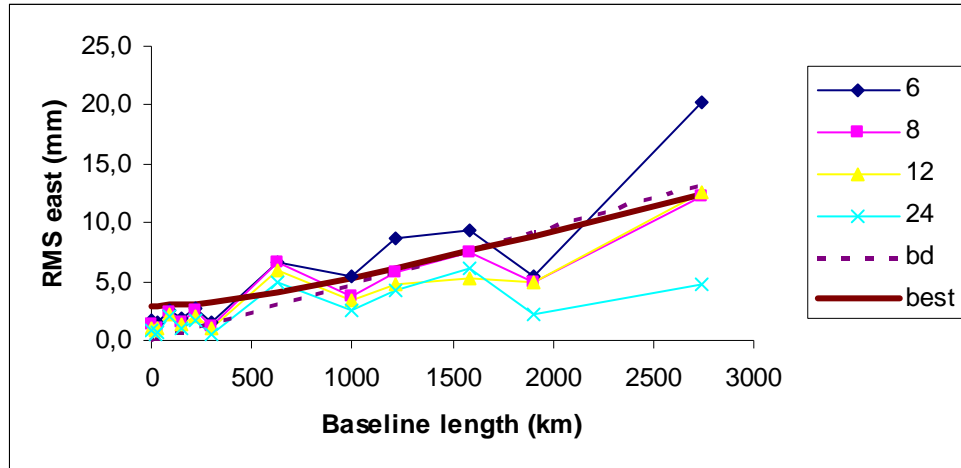


Figure 7.3.3. RMS errors and curves fit according to LSE for the east component

For east component Equation (7.3.1) is replaced by

$$S_e(L, T) = [a_e / T + d_e L^2]^{0.5} \rightarrow S_e = \sqrt{\frac{78.568}{T} + 19.46 \times 10^{-6} L^2} \quad (7.3.9)$$

where a and d are the significant coefficients for east component which fits best into our solutions. The results are the RMS values, expressed in mm.

In the Figures 7.3.1, 7.3.2 and 7.3.3, the dashed line shows the RMS values, when the coefficients b and d , which were found to be significant from the first LS analysis, are taken into consider. The solid line is created when a and b for north and up components, and a and d for east component are used for the calculation of the RMS values which fits best into our solutions. For both solid and dashed lines T is taken 9 hours as middle value.

Table 7.3.1. Mean RMS values for alternative coefficient combinations for all three GPS baseline components north, east and up

	RMS North (mm)	Sn (b-d) (mm)	Sn (b) (mm)	Sn (a-b) (mm)	Sn (a-d) (mm)	Sn (b-c) (mm)	Eckl Sn (a-b)
6 hr	4.0	2.9	3.3	4.1	4.2	3.6	2.6
8 hr	3.3	2.4	2.8	3.6	3.8	3.3	2.3
12 hr	2.6	1.8	2.3	2.9	3.4	3.0	1.9
24 hr	1.8	0.7	1.6	2.1	2.8	2.5	1.3
	RMS East (mm)	Se (b-d) (mm)	Se (b) (mm)	Se (a-b) (mm)	Se (a-d) (mm)	Se (b-c) (mm)	Eckl Sn (a-d)
6 hr	5.3	4.8	5.3		5.5		3.7
8 hr	4.0	4.0	4.6		5.1		3.3
12 hr	3.6	3.0	3.8		4.7		2.7
24 hr	2.5	1.3	2.7		4.2		2.0
	RMS Up (mm)	Su (b-d) (mm)	Su (b) (mm)	Su (a-b) (mm)	Su (a-d) (mm)	Su (b-c) (mm)	Eckl Su (a-b)
6 hr	13.4	10.1	11.3	14.3	14.5	12.7	9.1
8 hr	11.3	8.3	9.8	12.4	13.2	11.6	7.9
12 hr	8.7	6.1	8.0	10.1	11.7	10.3	6.5
24 hr	6.0	2.1	5.7	7.1	9.9	8.8	4.6

Table 7.3.2. Estimated values of constants in Equation (7.3.1)

Parameter (units)	Estimated value	Formal 1-sigma Uncertainty	<i>Ratio</i>
<i>an</i> ($\text{mm}^2.\text{h}$)	16.72	42.18	0.39
<i>ae</i> ($\text{mm}^2.\text{h}$)	-68.56	103.65	-0.66
<i>au</i> ($\text{mm}^2.\text{h}$)	22.59	612.05	0.04
<i>bn</i> ($\text{ppb}^2.\text{h}$)	107.78	17.08	6.31
<i>be</i> ($\text{ppb}^2.\text{h}$)	307.04	42.00	7.31
<i>bu</i> ($\text{ppb}^2.\text{h}$)	1327.76	248.18	5.35
<i>cn</i> (mm^2)	2.82	4.81	0.58
<i>ce</i> (mm^2)	8.27	11.83	0.70
<i>cu</i> (mm^2)	55.66	69.84	0.80
<i>dn</i> (ppb^2)	-44.78	19.55	-2.29
<i>de</i> (ppb^2)	11.04	-4.80	-2.30
<i>du</i> (ppb^2)	-59.27	28.36	-2.09

Table 7.3.3. Mean RMS for all 13 baselines

T (hour)	North (Sn) (mm)	East (Se) (mm)	Up (Su) (mm)
6	4.0 (4.1)	5.3 (5.5)	13.4 (14.3)
8	3.3 (3.6)	4.0 (5.1)	11.3 (12.4)
12	2.6 (2.9)	3.6 (4.7)	8.7 (10.1)
24	1.8 (2.1)	2.5 (4.2)	6.0 (7.1)

Table 7.3.3 compares the values computed from Equations (7.3.7), (7.3.8), (7.3.9) with the mean RMS values for all 13 baselines for each dimension and each value of T . The first values in the table show the mean RMS values whereas the values in the parenthesis are the mean standard errors computed for our model. Both values are in mm degree.

8. CONCLUSION

GPS accuracy assessment was made for 13 baselines ranging from 3 to 3000 km, each connecting a pair of IGS stations. 10 days of data for each baseline, downloaded from SOPAC website, have been processed by using GIPSY software. The relation among GPS point positioning, base length and duration of observation has been examined and least square estimation was made to define a unified model for our data range.

Previously published LS functional models were adopted and their effect on GPS baseline processing results for both long and short baselines was investigated. Standard errors for these scales could be obtained by using the equations

$$S_n = \sqrt{\frac{39.3}{T} + \frac{71.96 \times 10^{-6} L^2}{T}} \quad (8.1)$$

$$S_e = \sqrt{\frac{78.568}{T} + 19.46 \times 10^{-6} L^2} \quad (8.2)$$

$$S_u = \sqrt{\frac{467.846}{T} + \frac{853.57 \times 10^{-6} L^2}{T}} \quad (8.3)$$

where S_n , S_e and S_u are the standard errors for north, east and up directions respectively. S_n , S_e and S_u values are expressed in mm, L is expressed in km and T is expressed in hours.

We can conclude that GPS positioning accuracy over short and long baselines depends both on the observing session duration and the baseline length. It is possible to define a unified model for this range. According to Eckl *et al.*, (2001) the empirical prediction formulas derived for shorter baselines (*i.e.* baselines shorter than 300 km) show some agreement in determined confidence intervals for baselines up to 2000 km. However, the formulas created as a result of our study are for a wider data range (*i.e.* baselines

ranging from 3 to 3000 km) and can be used to compute the standard errors for both short and long baselines.

REFERENCES

- Blewitt, G., 1989, "Carrier Phase Ambiguity Resolution for the Global Positioning System Applied to Geodetic Baselines up to 2000 km", *Journal of Geophysical Research*, Vol: 94(B8), pp:10187-10283.
- Blewitt, G., 1997, "Basics of GPS Technique: Observation Equations in Geodetic Applications of GPS", ed. B. Johnson, *Nordic Geodetic Commission*, Sweden, ISSN 0280-5731, pp: 10-54.
- Blewitt, G., 2008, "Fixed Point Theorems of GPS Carrier Phase Ambiguity Resolution and Their Application to Massive Network Processing", *Journal of Geophysical Research*, Ambizap, 113, B12410, doi:10.1029/2008JB005736.
- Dogan, U., 2007, "Accuracy Analysis of Relative Positions of Permanent GPS Stations in the Marmara Region, Turkey", *Survey Review*, Vol: 39 (304), pp:156-165.
- Eckl, M.C., Snay, R.A., Soler, T., Cline, M.W., and G.L. Mader, 2001, "Accuracy of GPS-derived Relative Positions as a Function of Inter-station Distance and Observing Session Duration", *Journal of Geodesy*, Vol: 75, pp: 633-640.
- Engin C., and U. Sanli, 2009, "Accuracy of GPS Positioning over Regional Scales", *Survey Review*, 41-132, pp: 192-200.
- Gregorius, T., 2001, "GIPSY-OASIS II, How It Works", Department of Geomatics, University of Newcastle Upon Tyne, pp:152.
- King M., Edwards S. and P. Clarke, 2002, "Precise Point Positioning: Breaking the Monopoly of Relative GPS Processing", *Engineering Surveying Showcase*.
- Ozer, E., 2004, *GPS ile Uzun Bazların Değerlendirilmesinde Ölçüm Süresinin Baz Çözüm Duyarlılığı Üzerine Etkisi*, M.S. Thesis (in Turkish), Yıldız Technical University.

- Soler, T., Michalak, P., Weston, N.D., Snay, R.A., and R.H. Foote, 2005, "Accuracy of OPUS Solutions for 1- to 4-h Observing Sessions", *GPS Solutions*, Vol: 10, pp: 45-55.
- Stewart, M., and C. Rizos, 2002, "GPS Projects: Some Planning Issues", *Manual of Geospatial Science & Technology*, JD Bossler *et al.*, ed., Taylor and Francis, London and New York, pp: 162-182.
- Tralli, D.M., and S.M. Linchten, 1990, "Stochastic Estimation of Tropospheric Path Delays in GPS Geodetic Measurements", *Journal of Geodesy*, Vol: 64-2, pp: 127-159.
- Treuhaft, R.N., and G.E. Lanyi, 1987, "The effect of the Dynamic Wet Troposphere on Radio Interferometric Measurements", *Radio Science*, Vol: 22, pp: 251-265.
- Webb, F.H., and J.F. Zumberge, 1993, "An Introduction to GIPSY/OASIS II", *JPL Publ.*, D-11088, Jet Propulsion Laboratory, Pasadena, CA.
- Zumberge, J.F., Heflin, M.B., Jefferson, D.C., Watkins, M.M., and F.H. Webb, 1997, "Precise Point Positioning For the Efficient and Robust Analysis of GPS Data from Large Networks", *Journal of Geophysical Research*, Vol: 102, pp: 5005-5017.

AUTOBIOGRAPHY

Name Surname: Didem Öztürk

Date of Birth: 04/10/1982

Place of Birth: İzmit / Kocaeli

High School: Atafen High School / İzmit (1993-2000)

College: Yıldız Technical University / Geodesy and Photogrammetry Engineering (2000-2005)

Master's Degree: Bogaziçi University Kandilli Observatory and Earthquake Research Institute (2005-2009)